

KINETICS OF THE DESORPTION OF AMMONIA
FROM WATER BY DIFFUSED AERATION

By
Jerzy Patoczka

Thesis

Submitted to the Faculty of the
Graduate School of Vanderbilt University
in partial fulfillment of the requirements
for the degree of
MASTER OF SCIENCE

in

Environmental and Water Resources Engineering

August, 1983

Nashville, Tennessee

Approved:

Date:

ENVIRONMENTAL AND WATER RESOURCES ENGINEERING

KINETICS OF THE DESORPTION OF AMMONIA FROM WATER BY DIFFUSED AERATION

JERZY PATOCZKA

Thesis under the direction of Professor David J. Wilson

The purpose of this thesis is to determine factors governing the kinetics of ammonia desorption from water by diffused aeration.

Experimental work was preceded by the development of the theoretical basis for the operation. The formula was derived for the calculation of the fraction of ammonia present in the solution in the undissociated form (susceptible for desorption), for any given temperature and pH.

Ammonia desorption was experimentally investigated in a laboratory scale column. Air bubbles were introduced into a NH_4Cl solution, and rate of the decrease of ammonia concentration was recorded. Experiments were conducted at 25°C and pH 11.6. Effect of the bubble size and depth of diffuser submersion on the rate of ammonia removal were investigated.

The results of the experimental work indicate that ammonia desorption by diffused aeration is not mass transfer but equilibrium controlled. The air bubbles leaving the solution were saturated with ammonia for depths as little as 1.5 cm and bubbles as large as 6.1 mm.

This is in accordance with theoretical considerations, but is in disagreement with recent works in which authors correlate efficiency

of the ammonia desorption with depth of submersion of the diffuser, size of the bubbles and other hydrodynamic parameters of the system.

Values of the mass transfer coefficient, as estimated from the experimental results, are not in conflict with the ones theoretically predicted.

In calculations impact of the surface effect on the rate of desorption in the column was taken into account.

Approved _____
Adviser

Date _____

ACKNOWLEDGMENTS

The author wishes to express his gratitude to Dr. David J. Wilson, Professor of Chemistry for his direction and support during this study.

Appreciation is also extended to his academic adviser, Dr. Edward L. Thackston, Chairman of Environmental and Water Resources Engineering.

The author was financially supported during the completion of this project from Vanderbilt University.

TABLE OF CONTENTS

	Page
ACKNOWLEDGMENTS	ii
LIST OF TABLES	v
LIST OF FIGURES	vi
 Chapter	
I. INTRODUCTION	1
II. LITERATURE REVIEW AND OBJECTIVE	2
Nitrogen Control in Wastewater	2
Ammonia Removal by Desorption with Air	2
Ammonia Removal by Diffused Aeration	4
Objective	8
III. THEORETICAL BASIS OF AMMONIA DESORPTION	10
Equilibrium Constant	10
Chemistry of Ammonia in Water	13
Rate of Ammonia Desorption	15
IV. EXPERIMENTAL PROCEDURE	20
Experimental Set-Up	20
Method of Conducting Experiments	22
Methodology of Measurements	23
V. EXPERIMENTAL RESULTS	33
VI. DISCUSSION	47
Surface Effect	47
Effect of Bubbles Diameter and Contact Time on Rate of Ammonia Removal	47
Estimation of the Mass Transfer Coefficient	55
VII. CONCLUSIONS	59
 Appendix	
A. COMPUTER PROGRAM FOR PROCESSING OF EXPERIMENTAL DATA	61

	Page
B. DETAILED PARAMETERS AND RESULTS OF EXPERIMENTS	64
C. CALCULATIONS OF BUBBLE CONTACT TIME AND IT'S CORRELATION WITH SLOPE b	67
D. CALCULATION OF THE MASS TRANSFER COEFFICIENT	70
BIBLIOGRAPHY	76

LIST OF TABLES

Table		Page
1.	Comparison of Nitrogen Removal Processes	3
2.	Equilibrium Constant for Ammonia Solubility in Water at 25°C	11
3.	Ionization Constants of Ammonia K_1 and Ionic Product Constant of Water K_w	14
4.	Basic Parameters and Results of the Experiments. Runs 1-9 and 29, Fine Bubbles	39
5.	Basic Parameters and Results of the Experiments. Runs 10-15, Medium Bubbles	40
6.	Basic Parameters and Results of the Experiments. Runs 16-26 and 28, Coarse Bubbles	41
7.	Basic Results and Parameters of the Experiments with Surface Aeration	42
8.	Results of the Correlation Between Slope b and Contact Time	50
9.	Comparison of Theoretically Predicted and Obtained Values of Mass Transfer Coefficient	57

LIST OF FIGURES

Figure		Page
1.	Schematic of the Experimental Set-up	21
2.	Rotametr Calibration Curve	24
3.	Calibration Curves for Ammonia Concentration Measurments	26
4.	Increase of Water Level Due to Air Flow for Different Diffuser Submersions. Fine Bubbles, Air Flow 0.6 l/min	27
5.	Increase of water Level Due to Air Flow for Different Diffuser Submersions. Medium Bubbles, Air Flow 1.1 l/min	28
6.	Increase of Water Level Due to Air Flow for Different Diffuser Submersions. Coarse Bubbles, Air Flow 0.6 l/min	29
7.	Fine Bubble Formation in the Column	30
8.	Medium Bubble Formation in the Column	31
9.	Coarse Bubble Formation in the Column	32
10.	Means of Air-Water Contact in the Experiments with Surface Aeration	34
11.	Dependence Between Air to Water Volumetric Ratio and Degree of Ammonia Removal. Run No. 5	37
12.	Dependence Between Air to Water Volumetric Ratio and Degree of Ammonia Removal. Run No. 28	38
13.	Dependence of the Slope of the Correlation Equation on the Diffuser Submersions. Fine Bubbles, Flow 0.6 l/min	43
14.	Dependence of the Slope of the Correlation Equation on the Diffuser Submersions. Medium Bubbles, Flow 1.1 l/min	44

	Page
15. Dependence of the Slope of the Correlation Equation on the Diffuser Submersion. Coarse Bubbles, Flow 1.1 l/min	45
16. Dependence of the Slope of the Correlation Equation on the Diffuser Submersion. All Runs	46
17. Effect of the Bubbles Contact Time on the Efficiency of Ammonia Removal. Fine Bubbles, Flow 0.6 l/min	51
18. Effect of the Bubbles Contact Time on the Efficiency of Ammonia Removal. Medium Bubbles, Flow 1.1 l/min	52
19. Effect of the Bubbles Contact Time on the Efficiency of Ammonia Removal. Coarse Bubbles, Flow 0.6 l/min	53

CHAPTER I

INTRODUCTION

Man's activity causes an increase in the nitrogen level in the aquatic environment. Sources of this nitrogen include domestic, industrial and animal farm wastes, rural and urban runoff and rainfall. Major forms of nitrogen in water and wastewater are: ammonia-nitrogen, nitrite-nitrogen, nitrate-nitrogen and organic nitrogen. Organic compounds containing nitrogen usually undergo bio-hydrolysis in water with subsequent release of ammonia [1].

Excessive amounts of various forms of nitrogen have a deleterious effect on water quality. This includes depletion of dissolved oxygen levels, stimulation of aquatic growth, toxicity to aquatic life, deterioration of chlorine disinfection efficiency and limitation of suitability of wastewater for reuse [1]. In the last two decades growing public awareness of environmental issues, as well as economic considerations, have caused extensive development of processes for nitrogen removal from wastewater, which is most easily controlled as a point source.

CHAPTER II

LITERATURE REVIEW AND OBJECTIVE

Nitrogen control in wastewater

Conventional wastewater treatment plants (without nitrification) have only limited capacity for nitrogen removal. Plant effluents thus contain large concentrations of nitrogen with ammonia nitrogen concentration being generally in the range 10- 30 mg/l (as N) [1,2,3,4]. Several technically and economically feasible methods are available to reduce this concentration. They are listed and characterized in Table 1.

It should be noted that the relative costs of the treatment processes listed in Table 1 are controversial, and some authors claim that ammonia desorption is by far the least expensive nitrogen removal process [3]. Low cost and other advantages of this process (Table 1) make it an attractive alternative, particularly where atmospheric conditions are favorable and when it is used in conjunction with high-lime phosphorus removal.

Ammonia removal by stripping with air

Desorption of ammonia from wastewater occurs when liquid of high pH is brought into contact with large amounts of air. There are several possible designs of providing air-water contact in order to desorb ammonia. These includede:

TABLE 1

COMPARISON OF NITROGEN REMOVAL PROCESSES

Process	Advantages	Disadvantages	Efficiency [1] %	Relative Cost [2]
Biological Nitrification- Denitrification	<ul style="list-style-type: none"> - N₂ end Product - all Forms of nitrogen removed 	<ul style="list-style-type: none"> - long detention time - sensitive to inhibitors changing flow and temperature 	70 - 95	1.00
Breakpoint chlorination	<ul style="list-style-type: none"> - complete removal can be obtained - temperature variation and inhibition proof 	<ul style="list-style-type: none"> - chemicals added increase greatly TDS - dechlorination often is necessary - continuous control equipment required 	90-100	-
Ammonia Stripping	<ul style="list-style-type: none"> - simplicity of operation - ease of control - no by products 	<ul style="list-style-type: none"> - scale formation - inefficient in low temperatures 	50 - 95	1.32
Selective ion exchange on clinoptilolite	<ul style="list-style-type: none"> - temperature change and inhibition proof 	<ul style="list-style-type: none"> - by product formation (brine) 	90 - 97	1.54

1. Countercurrent or crosscurrent stripping towers with stationary bed,
2. Stripping ponds (with and without agitation),
3. Spray towers,
4. Diffused aeration,
5. Three-phase fluidized bed.

Considerable laboratory and pilot-scale data on the three first methods are available in the literature [3,4,5,6,7,8]. The operation of stripping towers is particularly well documented, and these have found application in several full-scale water reclamation plants [9,10,11]. The available literature data on ammonia desorption by diffused aeration are very limited and, moreover, contradictory results have been reported on the role of hydrodynamic factors on the efficiency of this process.

Ammonia removal by diffused aeration

The possibility of ammonia desorption from wastewater by diffused aeration was first considered by Downing in 1958. He predicted [12] a low rate of ammonia removal when in contact with limited amounts of air (diffused aeration, surface agitation). In other words he stated indirectly that the removal process was equilibrium controlled. However, in the correlation of his experimental data he did not differentiate between mass-transfer and mass-balance effects and used the term "mass transfer coefficient" for the general reaction rate r defined as follows :

$$c = c_0 \cdot \exp(-r \cdot t) \quad (1)$$

where c_0, c = ammonia concentration $[ML^{-3}]$, initial and at time t $[T]$
 r = reaction rate $[T^{-1}]$

Such defined mass transfer coefficient turned out to be only a small fraction of the analogous mass transfer coefficient for oxygen adsorption in the same system.

Baley et al in 1967 [13] suggested that countercurrent systems are likely to be applied in ammonia desorption, since air can be better utilized in such systems.

The first experimental data on ammonia desorption by diffused aeration are available from the work by Benneworth and Morris [8]. They were unable to detect any decrease in the rate of desorption with decreasing water levels for depths as little as 1.5 cm [8]. Their conclusion, however, is not convincing, since calculations of the removal rate for smaller liquid depths were based on only two data points. Moreover, bubble diameter was not specified and solution temperature - an important factor - was not properly controlled. They stated "experiments were performed at room temperature which was reasonably constant at about 20°C".

The first major paper on ammonia desorption by diffused aeration was published by Srinath and Loehr in 1974. Authors initially stated [14] that air bubbles in the systems under consideration were almost instantaneously saturated with ammonia and an equilibrium constant can be used to estimate the quantity of the air needed for ammonia desorption. Nevertheless, in the equation describing mass-balance in a batch unit they used interfacial area A and mass transfer coefficient k

combined into an operational desorption coefficient K defined in the following form:

$$\ln \frac{c_1}{c_2} = K \cdot P \cdot (t_2 - t_1) \quad (2)$$

where c_1, c_2 = ammonia concentrations [ML^{-3}] at the times t_1, t_2

K = operational desorption coefficient ($K=k \cdot A$) [T^{-1}]

P = fraction of ammonia present in the solution as NH_3

Consequently, they used a desorption coefficient defined in this way for correlation of their data from small- and large-scale experiments in batch and continuous flow units. Effects of pH, temperature, viscosity, air flow rate and initial ammonia concentration on the value of K were investigated in numerous experiments. Values for K , obtained over a temperature range 10-30 °C, were correlated in the following form:

$$K = a \cdot (\mu)^b \quad (3)$$

where μ = viscosity [centipoises]

a = value of K when μ is 1 centipose (depends on air flow rate)

b = constant

K values obtained from their experiments ranged from 0.004 to 0.8/hr. In conclusion the authors stated that for designing purposes the mass transfer coefficient for diffused aeration should be determined experimentally for a particular system or estimated from semi-empirical relationships provided in the paper.

A mathematical model which describes the role of hydrodynamic conditions on the efficiency of ammonia desorption by diffused aeration was developed by Shpirt in a paper published in 1981 [15]. Experimental results were correlated in the following form:

$$K_L a = \frac{A \cdot D}{d^{1.25} \cdot \gamma^{0.45}} \cdot G^{0.45} \cdot h^{-0.30} \quad (4)$$

where $K_L a$ = overall mass transfer coefficient defined for batch operation as:

$$K_L a = \frac{\ln \frac{c_1}{c_2}}{t_2 - t_1} \quad [T^{-1}] \quad (5)$$

c_1, c_2 = ammonia concentrations $[ML^{-3}]$ at time t_1, t_2

D = coefficient of diffusivity $[L^2T^{-1}]$

d = diameter of air bubbles $[L]$

h = diffuser submersion $[L]$

G = air loading rate $[L^3L^{-2}T^{-1}]$

γ = kinematic viscosity $[L^2T^{-1}]$

A = constant

For two particular diffused air systems studied by the author, the obtained relationships were as follows:

$$K_L a = 7 \cdot 10^{-3} \cdot G^{0.45} \cdot h^{-0.30} \quad (6)$$

for coarse bubble system, and

$$K_L a = 13.6 \cdot 10^{-3} \cdot G^{0.45} \cdot h^{-0.30} \quad (7)$$

for a fine bubble system. Depth of diffuser submersion ranged from 30 to 100 cm, temperature = 20°C, pH = 11.5 ($K_L a = \text{hr}^{-1}$, $G = \text{m} \cdot \text{hr}^{-1}$, $h = \text{m}$).

The conclusion drawn by the author was that the mass transfer coefficient for ammonia desorption in diffused aeration systems was a function of hydrodynamic variables; namely depth of submersion of the diffuser, turbulence, and size of the air bubbles. Specifically the author found fine bubble aeration to be twice as efficient as coarse bubble aeration.

The review of the literature presented indicates that there is a basic contradiction between cited authors. Theoretical considerations and experimental data provided by some authors show that ammonia desorption by diffused aeration is equilibrium controlled and rate of removal can be calculated directly from mass balance [8,12]. Others found hydrodynamic conditions such as bubble diameter, viscosity and depth of submersion of importance [14,15].

Objective

The objectives of this work are to determine factors governing the kinetics of ammonia desorption by diffused aeration and to evaluate the mass transfer coefficient in this system. To accomplish this goal the following procedures are to be carried out:

1. Development of the theoretical basis for the operation,

2. Experimental investigation of the effect of the bubble size and bubble contact time on the rate of ammonia removal in the laboratory scale, batch mode apparatus. Experiments are to be carried out at 25°C and pH 11.6,
3. On the basis of the experimental results the problem of whether the process is equilibrium or mass transfer controlled will be addressed,
4. In case significant mass transfer effects are noted, the mass transfer coefficient will be evaluated and compared with theoretical predictions.

CHAPTER III

THEORETICAL BASIS OF AMMONIA DESORPTION

Equilibrium constant

The relationship between ammonia concentration in water and its partial pressure above the solution is well established for concentrations above 1000 mg/l. For lower concentrations, which are of interest in wastewater treatment, values of the equilibrium constant for different temperatures can be calculated by extrapolation, assuming that Henry's law is valid for such small concentrations. Values of the equilibrium constant (at 25°C), gathered from available sources or calculated from raw data are given in Table 2. From the results of the experiments on ammonia stripping [5,9,11], the equilibrium constant can be estimated and it is in agreement with the values given in Table 2.

For the purpose of this study, it was necessary to develop a mathematical formula describing the dependence of the equilibrium constant on temperature in a narrow temperature range around 25°C. Basic for such a relationship is the Classius-Clapeyron equation:

$$\frac{dp}{dT} = \frac{P \cdot \Delta H_v}{R \cdot T^2} \quad (8)$$

where p = partial pressure of the gas

T = temperature in °K

R = gas constant

TABLE 2
EQUILIBRIUM CONSTANT FOR AMMONIA SOLUBILITY
IN WATER AT 25°C

Source	K*	$\frac{H^{**}}{[atm]}$ g/l
Locke, T. et al 1904 [21]	7.19×10^{-4}	10.33×10^{-4}
De Wijs 1923 [18]	6.94×10^{-4}	9.97×10^{-4}
Chemical Engineers Handbook 1964 [20]	7.00×10^{-4}	10.05×10^{-4}
Roesler, T.F. et al 1971 [19]	6.17×10^{-4}	8.86×10^{-4}

*K is defined as $K = c_g/c_L$

where C_g - ammonia concentration in the gas phase [g/l]

C_L = ammonia concentration in the solution [g/l]

**H is defined as $p = H \cdot C_L$

where p = partial pressure of ammonia [atm]

C_L = ammonia concentration in the solution [g/l]

ΔH_v = enthalpy of evaporation

Integration of Equation 8 yields

$$p = p_0 \cdot \exp \left[\frac{\Delta H_v}{R \cdot T \cdot T_0} \cdot (T - T_0) \right] \quad (9)$$

where p_0 = partial pressure at reference temperature T_0

Since $T_0 \approx T = 298^\circ\text{K}$, substitution into Equation 9 yields

$$p = p_0 \cdot \exp \left[B \cdot (T - T_0) \right] \quad (10)$$

where B = constant

This theoretical formula for the partial pressure of ammonia over liquid ammonia has been verified with available experimental data for the dilute solutions of ammonia in water. Verification based on data from the temperature range $21 - 32^\circ\text{C}$ [17] has given the final formula

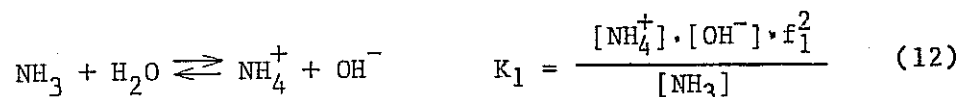
$$p = p_0 \cdot \exp \left[0.04473 \cdot (t' - 25) \right] \quad (11)$$

where t' = temperature in $^\circ\text{C}$

This formula was used in processing the experimental data to correct for the small temperature fluctuations around the designated operational temperature which occurred during our runs. It should be noted that the partial pressure of ammonia changes significantly with temperature. A temperature increase of 1°C (in the range $21 - 32^\circ\text{C}$) increases partial pressure of ammonia by 4.6%.

Chemistry of ammonia in water

Ammonia dissociates in water according to the following equation:



where brackets represent molar concentrations and f_1 = activity coefficient for monovalent ions. At neutral pH the reaction equilibrium is almost complete to the right in quite dilute solution. Since the ion activity product for water is

$$K_w = [\text{OH}^-] \cdot [\text{H}^+] \cdot f_1^2 \quad (13)$$

one can derive the following equation for the fraction P of ammonia present in NH_3 form, susceptible for desorption:

$$P = \frac{[\text{NH}_3]}{[\text{NH}_4^+] + [\text{NH}_3]} = \frac{1}{\frac{K_1}{K_w} \cdot 10^{-\text{pH} - \log(f_1)} + 1} \quad (14)$$

Values for the constants K_1 and K_w are given in Table 3. Graphs illustrating the relationship P versus temperature and pH have been prepared on the basis of the above equation (assuming $f_1 = 1$) and are available in many sources [1,14,19].

To provide an ample tool for quick calculation of P for any given pH in the temperature range 5 - 25°C, the constants K_1 and K_w were correlated with the temperature t' (°C) with the following results:

TABLE 3

IONIZATION CONSTANTS OF AMMONIA K_1
AND IONIC ACTIVITY PRODUCT CONSTANT FOR WATER K_w

Temperature °C	K_1 [18]	K_w [16]
5	1.479×10^{-5}	1.845×10^{-15}
10	1.570×10^{-5}	2.917×10^{-15}
15	1.652×10^{-5}	4.508×10^{-15}
20	1.710×10^{-5}	6.808×10^{-15}
25	1.774×10^{-5}	1.007×10^{-14}

$$\log(K_w) = t' \cdot 0.0039 - 4.85 \quad (15)$$

$$\log(K_1) = t' \cdot 0.0386 - 14.91 \quad (16)$$

These linear correlations approximate values of K_w and K_1 (in the above indicated range) with sufficient accuracy for all practical purposes.

Combination of Equations 14, 15 and 16 yields the final formula:

$$P = \frac{1}{1 + 10^{10.06 - \text{pH} - t' \cdot 0.0329 - \log(f_1)}} \quad (17)$$

This formula is valid for the temperature range encountered in wastewater treatment practise (5 - 25°C) and for any pH. For the average wastewater, value of activity coefficient for monovalent ions (f_1) can be estimated as equal to 0.9 and thus $\log(f_1) = 0.05$.

Rate of ammonia desorption

In order to develop a mathematical formula for the rate of ammonia removal from a batch reactor, let us first consider the mass balance in one bubble rising through the liquid layer. It may be assumed that in the short time required for the bubble to rise through the water, the concentration of ammonia remains constant in the water and that it is uniform throughout the column. Change in the mass of ammonia in the bubble is described by the following formula:

$$\frac{dm}{dt'} = F \cdot d' \cdot (c_g^* - c_g) = F \cdot d' \cdot (c \cdot K \cdot P - c_g) \quad (18)$$

where m = mass of ammonia in the bubble [M]

τ' = time [T]

F = surface area of the bubble [L^2]

α = mass transfer coefficient (based on gas phase) [LT^{-1}]

c_g = ammonia concentration in the bubble at time τ' [ML^{-3}]

c_g^* = equilibrium concentration of ammonia in the bubble in contact with solution having ammonia concentration c [ML^{-3}]

c = concentration of ammonia in the liquid ($NH_4^+ + NH_3$) [ML^{-3}]

P = fraction of the ammonia present in the solution as NH_3

$K = \frac{c_g^*}{c} = \text{equilibrium constant}$

For a bubble of diameter d

$$dm = dc_g \cdot \frac{\pi d^3}{6}, \quad F = \pi \cdot d^2 \quad (19)$$

Substitution into Equation 18 yields

$$\frac{dc_g}{K \cdot P \cdot c - c_g} = - \frac{6 \cdot \alpha \cdot d \tau'}{d} \quad (20)$$

Integration from time 0 to τ gives

$$\ln \frac{K \cdot P \cdot c - c'_g}{K \cdot P \cdot c} = - \frac{6 \cdot \alpha \cdot \tau}{d} \quad (21)$$

where c'_g = final concentration in the bubble as it leaves the water

τ = residence time of the bubble [T]

Rearrangement and substitution $\frac{6\pi r^2}{d} = a$ gives a formula for the ammonia concentration in a bubble leaving the water

$$c'_g = c \cdot K \cdot P \cdot \left[1 - \exp(-a \cdot \tau) \right] \quad (22)$$

The change of the ammonia concentration in the water is governed by the expression

$$- \frac{dc}{dt} \cdot V = c'_g \cdot Q \quad (23)$$

where $V =$ reactor volume $[L^3]$

$Q =$ flow rate of the air as it leaves the column $[L^3T^{-1}]$

In examining the ammonia mass balance in the solution, ammonia desorbed from the free water surface should be taken into account. The change in ammonia concentration in the solution due to the ammonia desorption from the water surface can be described by the following formula:

$$-V \cdot \frac{dc}{dt} = A \cdot \alpha^1 \cdot (c_g^* - c_g'') = c \cdot K \cdot P \cdot s \cdot (1 - f) \quad (24)$$

where $c_g'' =$ ammonia concentration in the gas entering the space above the water surface $[ML^{-3}]$

$\alpha^1 =$ mass transfer coefficient for the free water surface $[LT^{-1}]$

$A =$ surface of the water-air interface $[L^2]$

$s = \alpha^1 \cdot A \quad [L^3T^{-1}]$

f = degree of saturation of the air entering the space over the water surface with respect to the bulk liquid ammonia concentration ($f = \frac{c_g''}{c_g}$)

The change in the mass of ammonia present in the solution due to the mass transfer from the bubble surface and from free water surface is additive. Therefore, on combining Equations 22, 23 and 24 we obtain

$$-V \cdot \frac{dc}{dt} = c \cdot K \cdot P \cdot [1 - \exp(-a \cdot \tau)] \cdot Q + c \cdot K \cdot P \cdot s \cdot (1 - f) \quad (25)$$

Integration of Equation 25 yields Equation 26 for the rate of ammonia removal

$$\ln \frac{c_0}{c} = \frac{Q \cdot t}{V} \cdot K \cdot P \cdot [1 - \exp(-a \cdot \tau) + s/Q(1 - f)] \quad (26)$$

where c_0 = initial ammonia concentration in the solution [ML⁻³]

For the air in a bubble reaching the water surface $c_g'' = c_g'$ and therefore from Equation 22 we obtain

$$f = 1 - \exp(-a \cdot \tau) \quad (27)$$

Substitution into Equation 26 gives

$$\ln \frac{c_0}{c} = \frac{Q \cdot t}{V} \cdot K \cdot P \cdot [1 - (1 - s/Q) \cdot \exp(-a \cdot \tau)] \quad (28)$$

In a given experiment Q, V, K, P, d, α, s and water level (thus τ) can be assumed to be constant. Therefore, change in ammonia concentration expressed in the form $\ln \frac{c_0}{c}$ should be directly proportional to the air to water volume ratio, with slope equal to $K \cdot P \cdot [1 - (1 - s/Q) \cdot \exp(-a \cdot \tau)]$

CHAPTER IV

EXPERIMENTAL PROCEDURE

Experimental set-up

Experiments were carried out in a laboratory scale desorption column. The experimental apparatus is illustrated in Figure 1.

The glass column was 5.2 cm in diameter and approximately 1 m high with a fine, fritted glass disc sealed at the bottom. An outlet port 1.5 cm above the bottom permitted rapid draining of the column and in part of the experiments it was used to insert a coarse or a medium sized bubble distributor made from plastic tubes perforated in the laboratory. A thermometer and a pH microelectrode (Fisher 1363994) were inserted into the column through two outlets located 24 and 30 cm above the bottom. Two sampling stopcocks were sealed into the column 0.5 and 54 cm above the frit. A third stopcock, located near the top of the column, was connected to the water U-manometer.

House air was passed through two diffused air scrubbers. The first one contained a H_2SO_4 solution to retain oily impurities from the air and to adsorb NH_3 which might be present in the air. The second scrubber contained NaOH solution. In it CO_2 was absorbed in order to prevent carbonate formation in the column and thus pH changes during the course of the experiments. It would also adsorb SO_3 released from the first scrubber. After leaving the column the air was passed through a soap film flow meter and control rotameter.

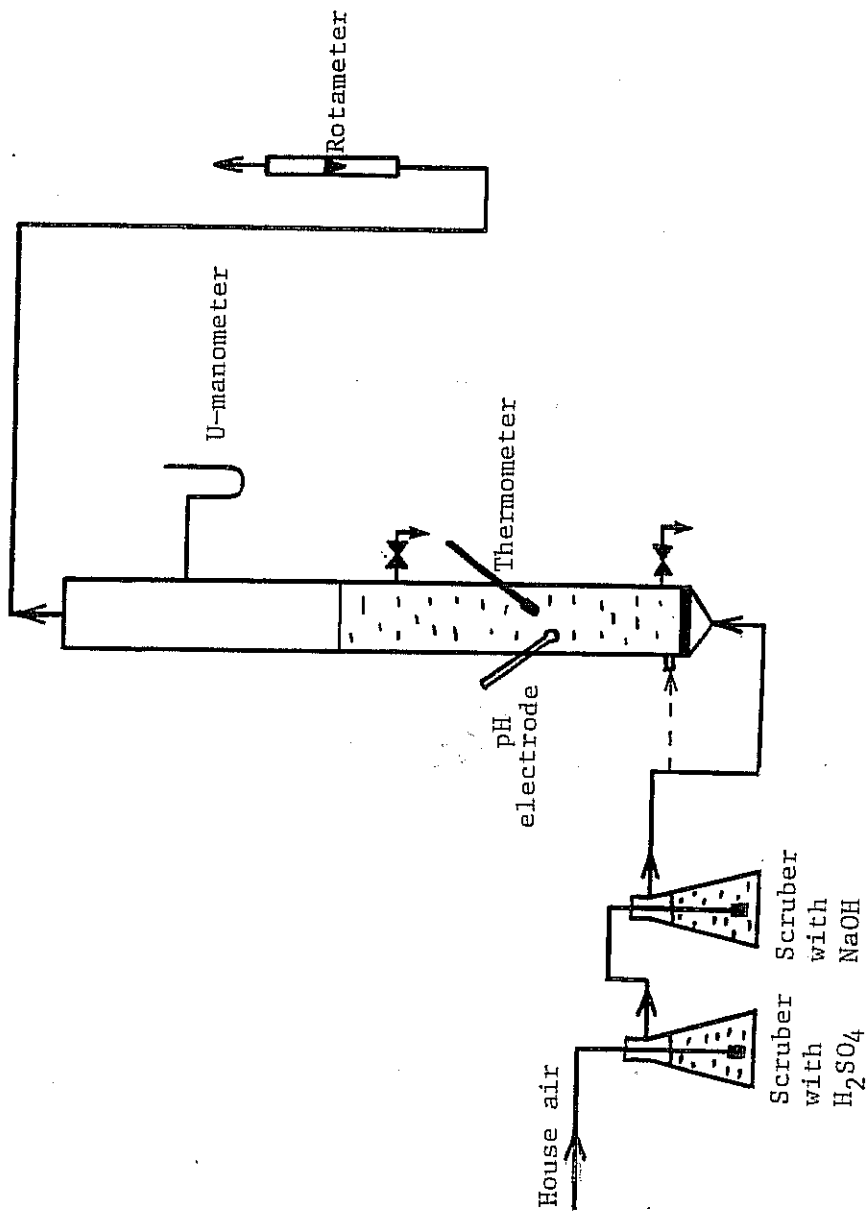


Figure 1. Schematic of the Experimental Set-Up

Method of conducting experiments

A stock solution of ammonium chloride (1000 mg/l as N) was prepared by dissolving anhydrous NH_4Cl (Fisher, certified ACS), dried at 100°C , in deionized water. Test solutions for each run were prepared by adding the desired amount of NH_4Cl stock solution to deionized water and then increasing the pH to 11.65 ± 0.05 with 0.5N NaOH solution. At this pH and the temperature 25°C virtually all ammonia (99.6%) was present in the NH_3 form. Initial ammonia concentrations ranged from 20 to 70 mg/l.

The required volumes of test solution (2 - 0.06 l) were measured with a volumetric flask and placed in the column giving a water height from 94.4 to 1.5 cm. After adjustments of the gas flow rate (in the range 0.27 - 1.35 l/min) the first sample was taken and the timing started. In each run usually 6 samples were taken at intervals designed to obtain approximately 3-fold decrease in ammonia concentration in the final sample. The experiments lasted from 4 to 72 hours, depending on water level and gas flow rate.

During each experiment gas flow rate, temperature and water level were monitored and recorded. In the initial experiments pH was continuously monitored to verify that the pH remained constant, and, thereafter it was checked only at the beginning and end of the experiments. Also the difference in pressure between column and atmosphere (resulting from head loss in tubing connecting the column and rotameter) was recorded.

Methodology of measurements

Air flow rate

Air flow rate was measured by Fisher & Porter Tri-Flat Variable-Area Precision Rotameters type FP-1/8-16-G-5/1/8-SA (flow range 0.1 - 1.4 l/min) and FP-1/16-20-G-5/1/16-SA (flow range 0.02-0.3 l/min). These rotameters were calibrated with a Precision Wet Test Meter (Precision Scientific Co.). The rotameter for the smaller flow range was also independently calibrated with a soap film flow meter. Both curves are in agreement (Figure 2). Experimental calibration curves for both rotameters are in turn in agreement with those provided by the manufacturer [20].

Since the flow rate was measured at atmospheric pressure (averaging around 750 mm Hg), proper corrections were made to determine the actual flow rate in the column using measurements of an open U-manometer connected to the top of the column.

Ammonia concentration

Samples were taken from the stopcock in a small beaker and measured with a pipet or a syringe. In some experiments, when the draining port was not used for air supply, samples were taken with a syringe directly from the column through the rubber stopper. Samples were then transferred to 25 ml volumetric flasks, diluted with deionized water, and sealed to avoid ammonia losses.

Determinations of the ammonia concentration were performed by the Direct Nesslerization Method [21]. Absorbance was measured on a U-2 Beckman Spectrophotometer at 420 μ m. Appropriate corrections for differences in optical characteristic of the cells were applied.

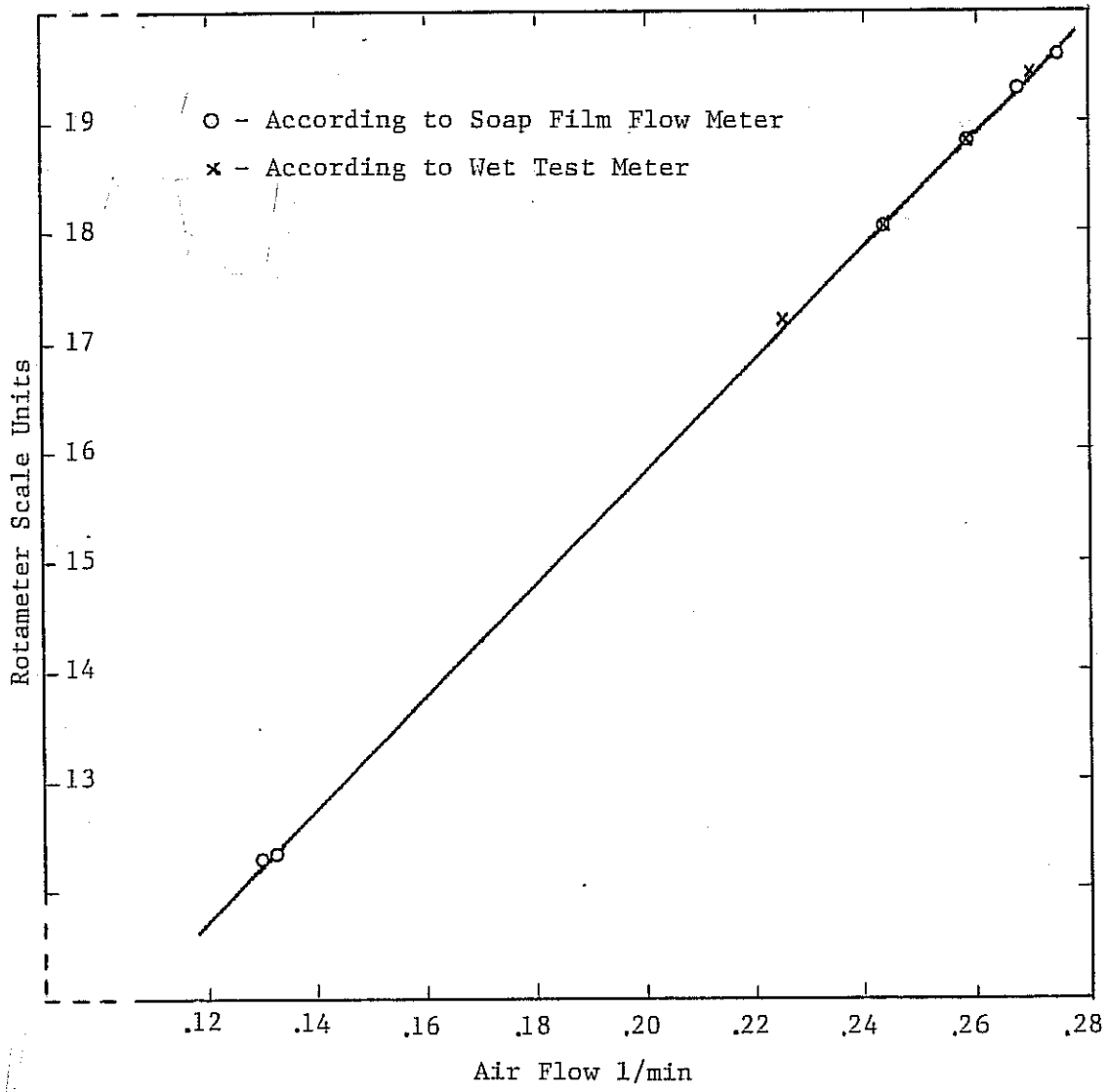


Figure 2. Rotameter Calibration Curve

Calibration curves were made for each new batch of reagents and best fitting formulas were used in processing the experimental data (Appendix A). Two typical calibration curves are given in Figure 3.

Temperature

Temperature was measured with 0.1 °C accuracy by a thermometer inserted into the column. The thermometer was calibrated with a Fisher ID 4270 Precision thermometer. In some experiments with low liquid level the thermometer was not immersed in water. However, this did not lead to wrong readings, since the temperatures of the water and of the air above the water surface were measured and found to be the same.

Bubble contact time and size

To determine the average bubble contact time, the level of water in the column was measured with and without air flow for different water levels and sizes of bubbles. From the results shown in Figures 4-6, the average bubble contact time was calculated for each water level and bubble size (detailed calculation and results are given in Appendix C).

In the above described experiments the height of the water levels included the surface bubble layer and thus the calculated contact times include the time when the bubble was sitting on the water surface before breaking.

The average size of bubbles for three types of diffuser were determined from photographs (Figures 7-9).

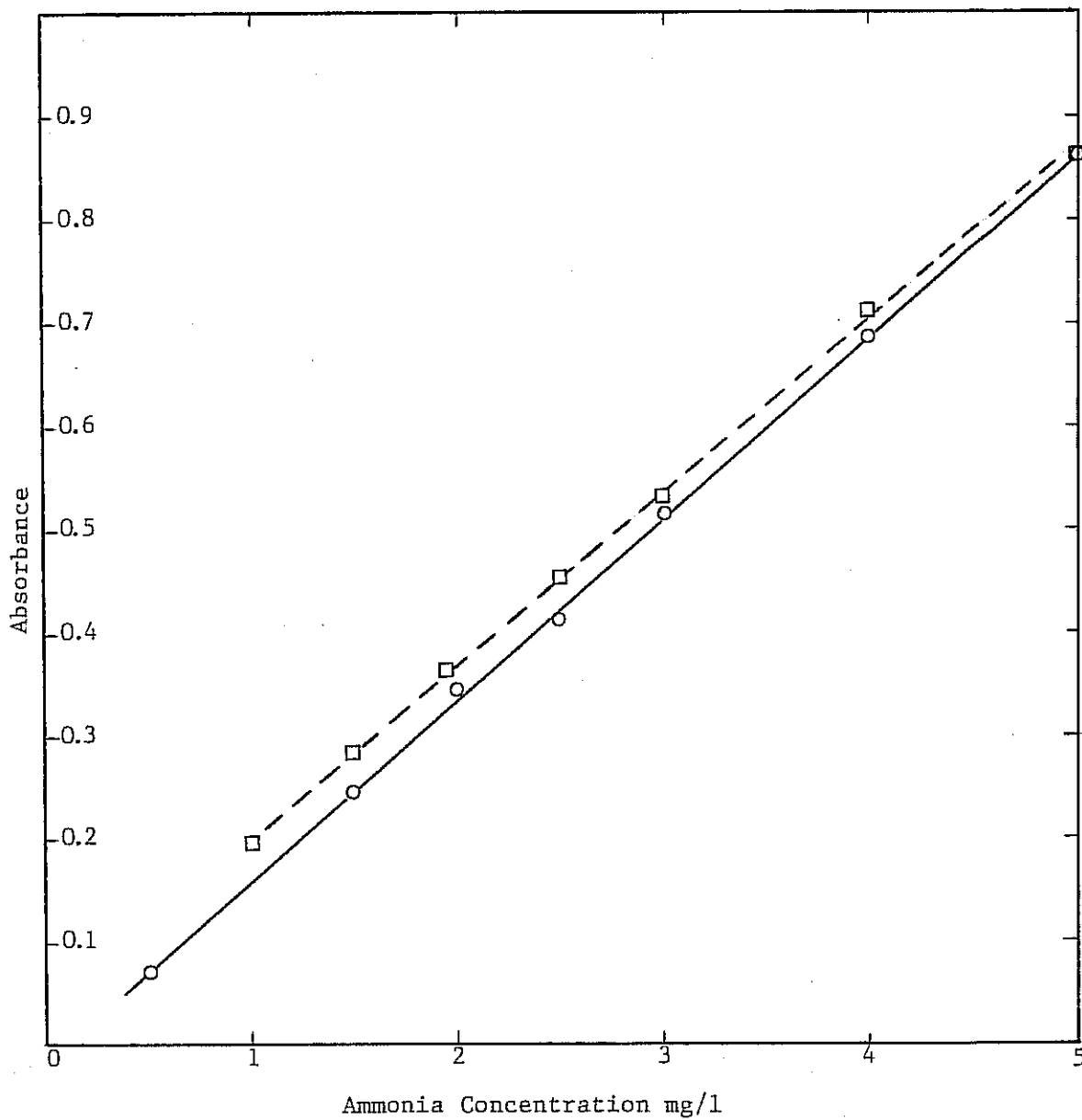


Figure 3. Calibration Curves for Ammonia Concentration Measurements

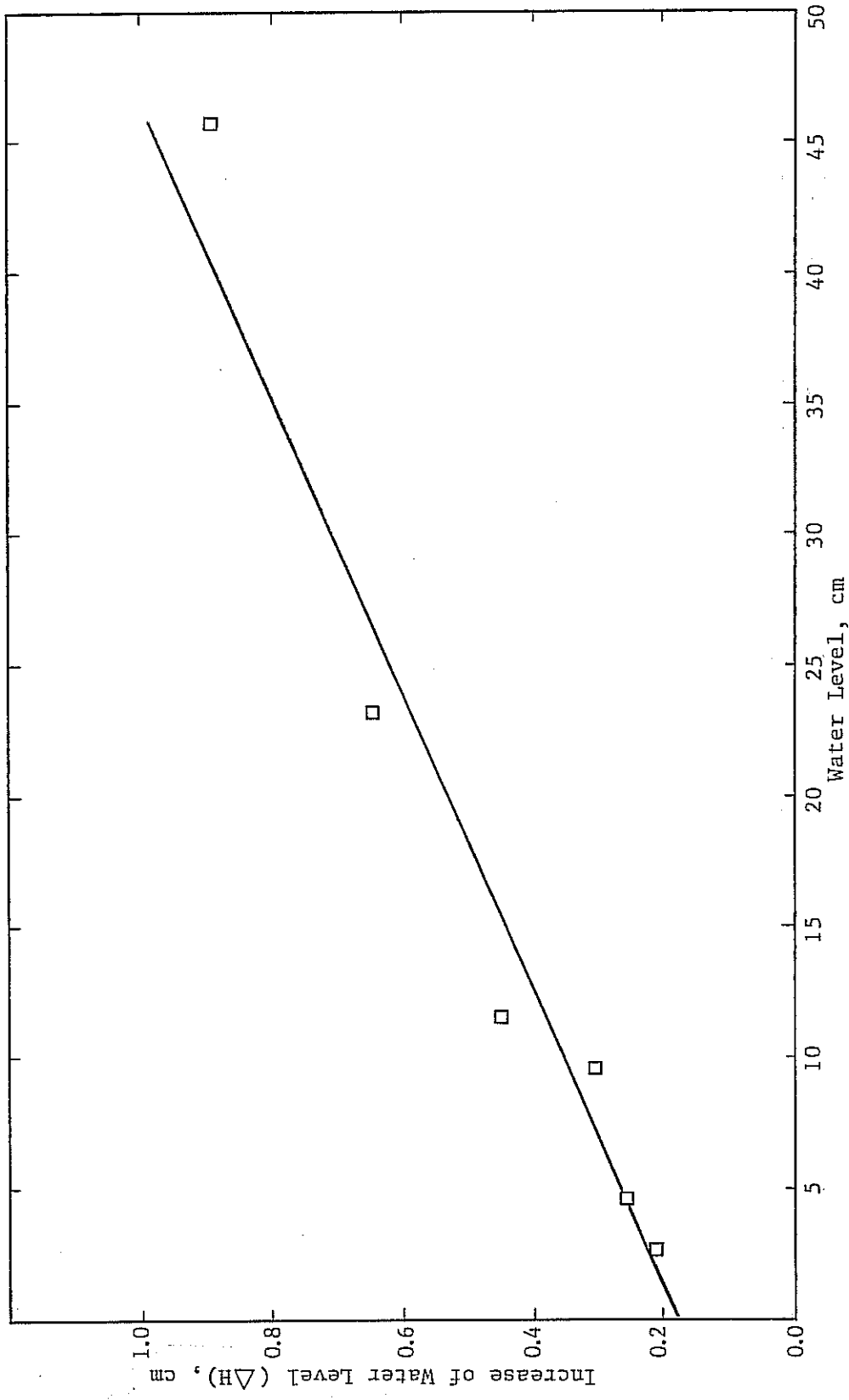


Figure 4. Increase of Water Level Due to Air Flow for Different Diffuser Submersion
Fine Bubbles, Air Flow 0.60 l/min

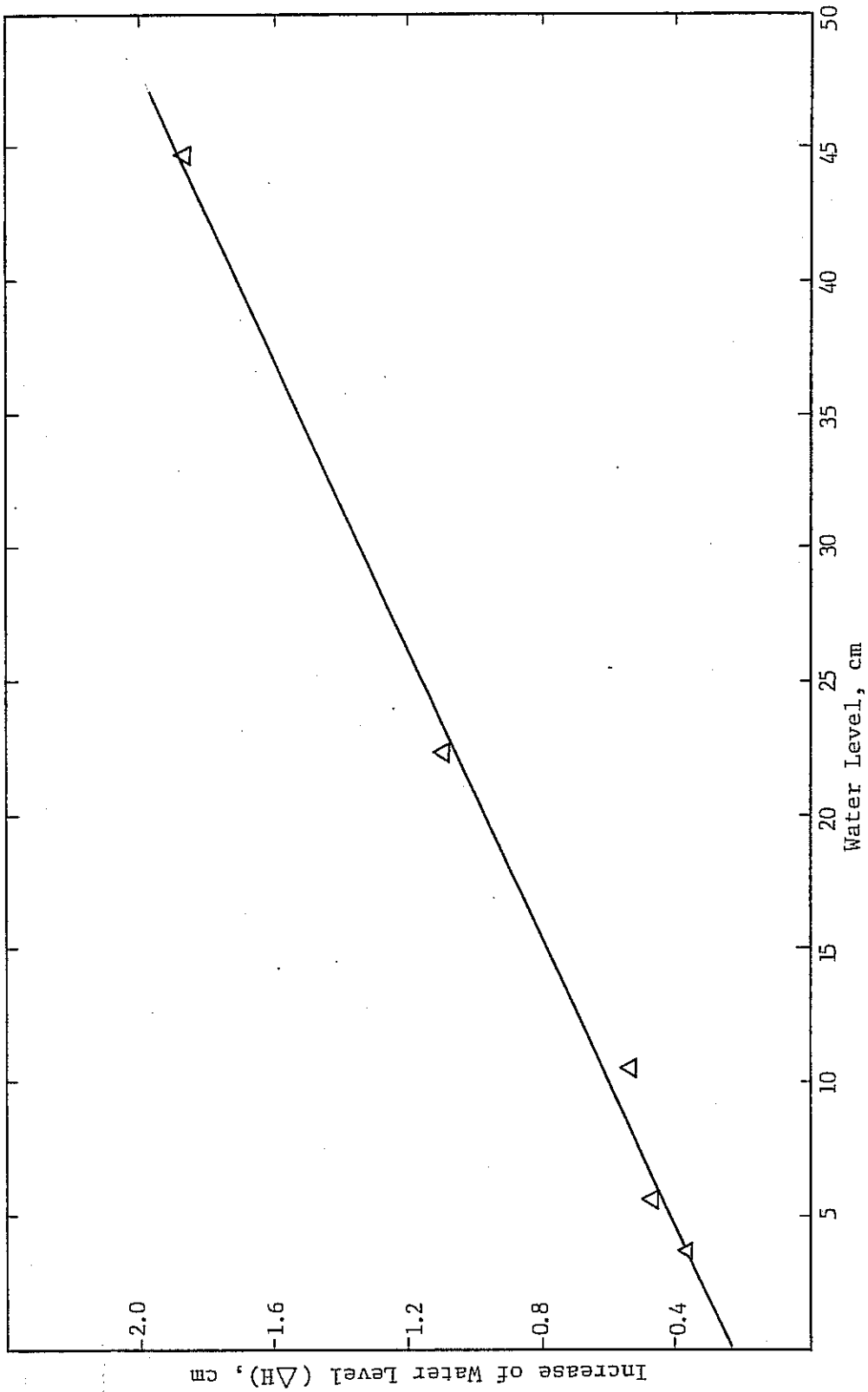


Figure 5. Increase of Water Level Due to Air Flow for Different Diffuser Submersion :
Medium Bubbles, Air Flow 1.1 l/min

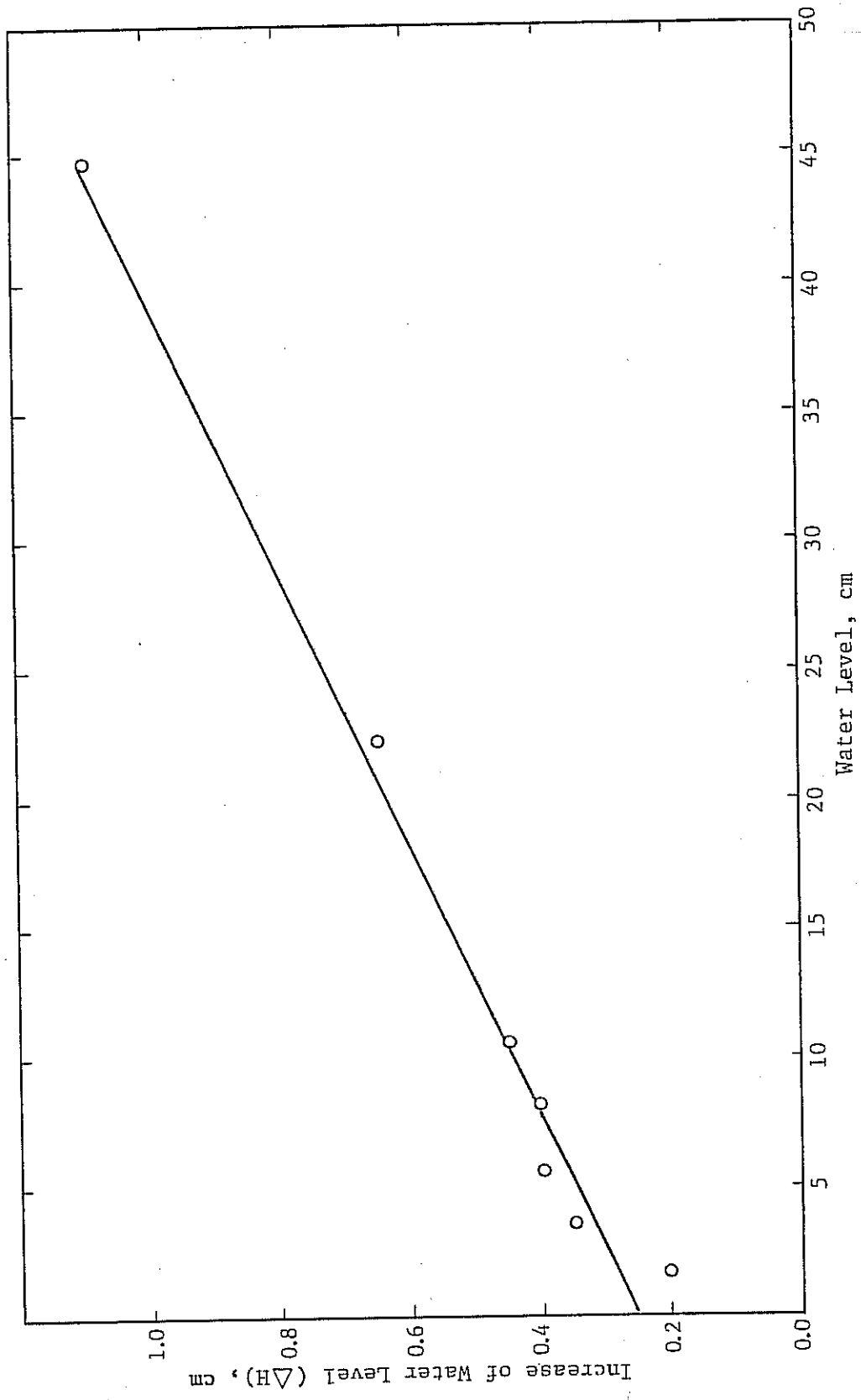


Figure 6. Increase of Water Level Due to Air Flow for Different Diffuser Submersion
Coarse Bubbles, Air Flow 0.60 l/min

Figure 7. Fine Bubble Formation in the Column

Figure 8. Medium Bubble Formation in the Column.

Figure 9. Coarse Bubble Formation in the Column

CHAPTER V

EXPERIMENTAL RESULTS

Thirty-one experiments were carried out with varying bubble diameter, air flow rate and water level. In runs no. 1-9 and 29 fine bubbles (average diameter 0.35 mm) from a fritted glass diffuser were used. In runs no. 10-15 bubbles with an average diameter of 4.1 mm from a perforated distributor were used, while in runs no. 16-26 and 28 coarse bubbles (6.2 mm) were applied.

In three additional runs (no. 27, 30 and 31) air was supplied to the column above the surface, rather than from the submerged diffuser. In run no. 31 air was released from a tube which touched the water surface, creating a bubble layer on the top of the liquid (see Figure 10a). In run no. 27 the end of the tube was not in contact with water but the contents of the column was continuously mixed (see Figure 10b). In run no. 30 air was released over a quiescent water surface (see Figure 10c).

Detailed parameters and results of the measurements for two exemplary runs (no. 3 and 4) are given in Appendix B.

By analogy with Equation 28, which describes change in ammonia concentration with time, the experimental data for each run were correlated in the following form:

$$\ln\left(\frac{c_0}{c}\right) = b\left(\frac{Q}{V} + t\right) \quad (29)$$

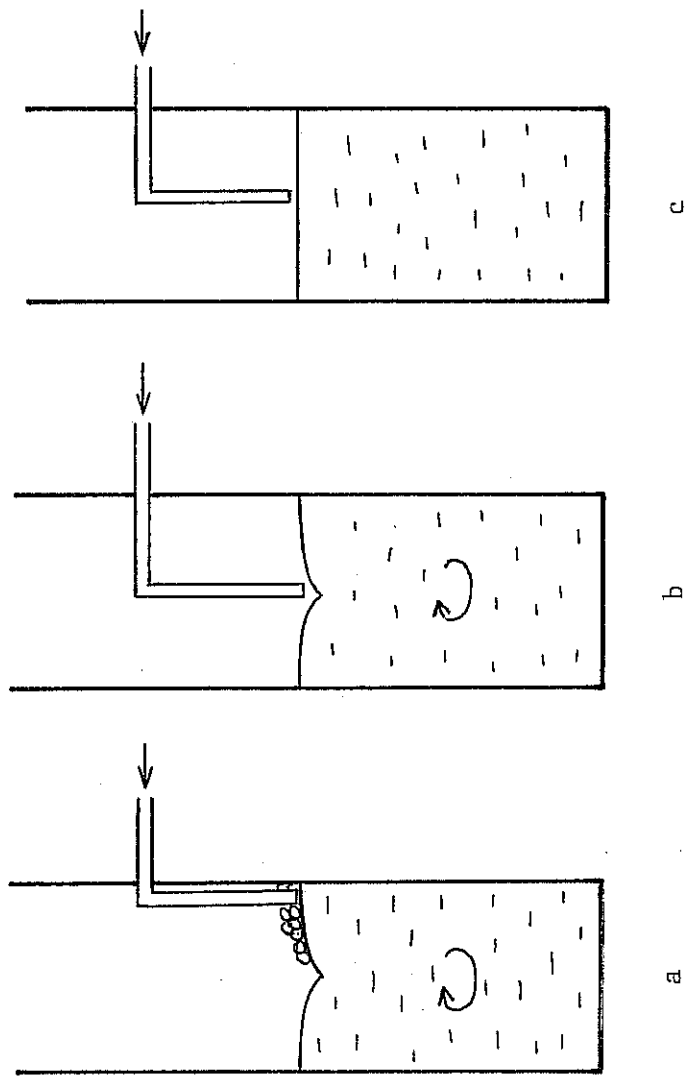


Figure 10. Means of Air-Water Contact in the Experiments with Surface Aeration

where b is constant for a given run.

The actual formula used for calculation of expression $\frac{Q_i t}{V}$ for each sampling interval i had the form

$$\frac{Q_i (t_i - t_{i-1})}{V_{i-1} - \Delta V} \cdot \frac{760 + \Delta P}{760} \cdot \exp \left[0.04473 (t_i' - 25) \right] \quad (30)$$

which includes corrections due to:

1. Changing volume of water in the column due to sampling, evaporation and leaks (ΔV),
2. Differences in pressure between the top of the column and the atmosphere (ΔP),
3. Small fluctuations of the water temperature t_i' during the course of the experiment.

Air to water volume ratios for each time interval were calculated from Equation 30 and subsequently added to give a cumulative air to water volume ratio Y , corresponding to decreasing ammonia concentration X . Results were computed using the program given in Appendix A. For two exemplary runs (no. 3 and 4) the values of X and Y calculated in the above described manner are given in Appendix B. For another two runs (no. 5 and 28) the values of X and Y are shown in Figures 11 and 12.

Slope b and statistical parameters of the correlation between X and Y were calculated for all runs with the Minitab statistical package. These values are listed in Tables 4-7 along with basic parameters for each run $\left(X = \ln \frac{c_0}{c} \right)$.

The slope (b) dependence on water level (contact time) for fine, medium and coarse bubbles is shown in Figures 13-16.

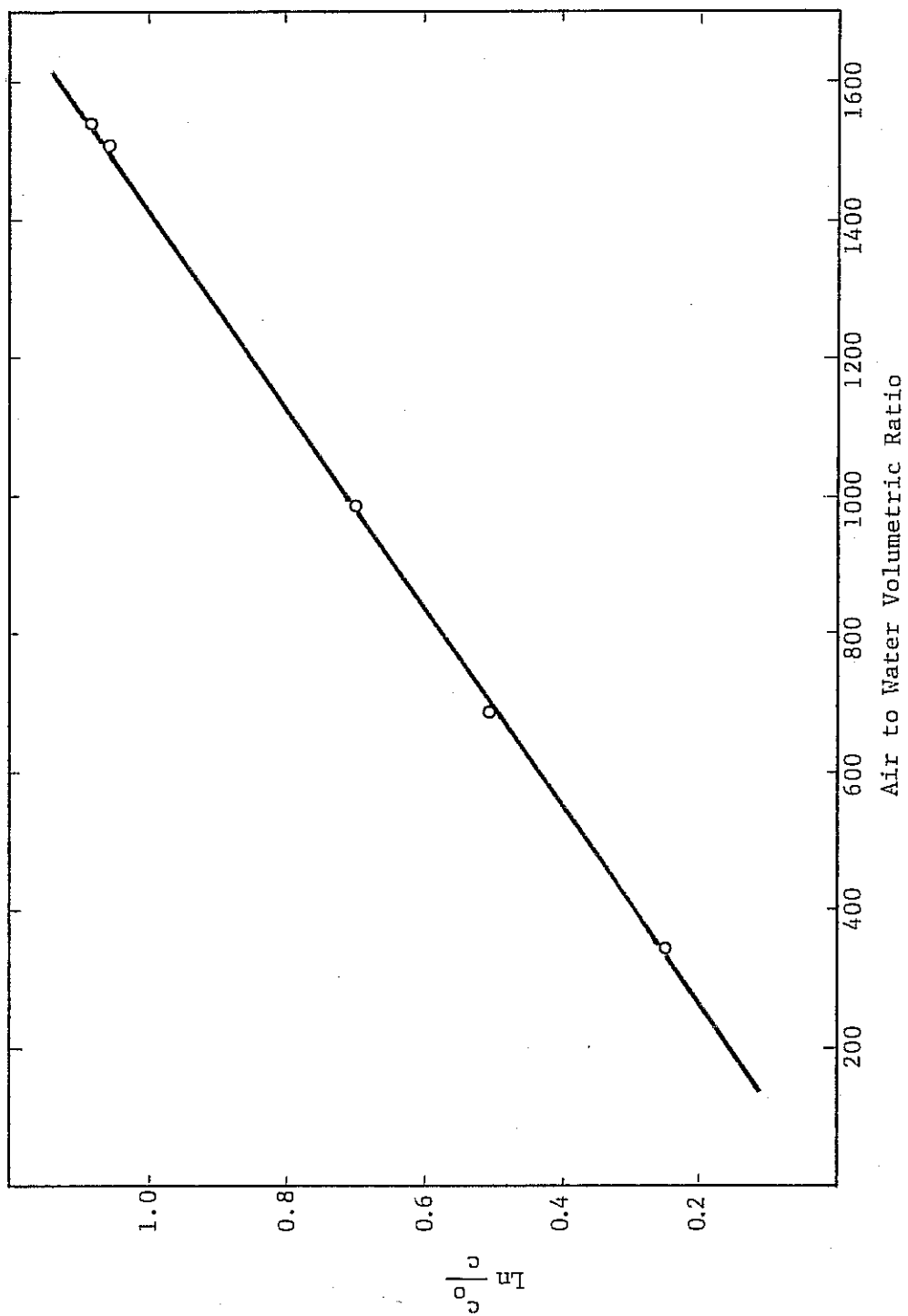


Figure 11. Dependence Between Air to Water Volumetric Ratio and Degree of Ammonia Removal (Run 5)

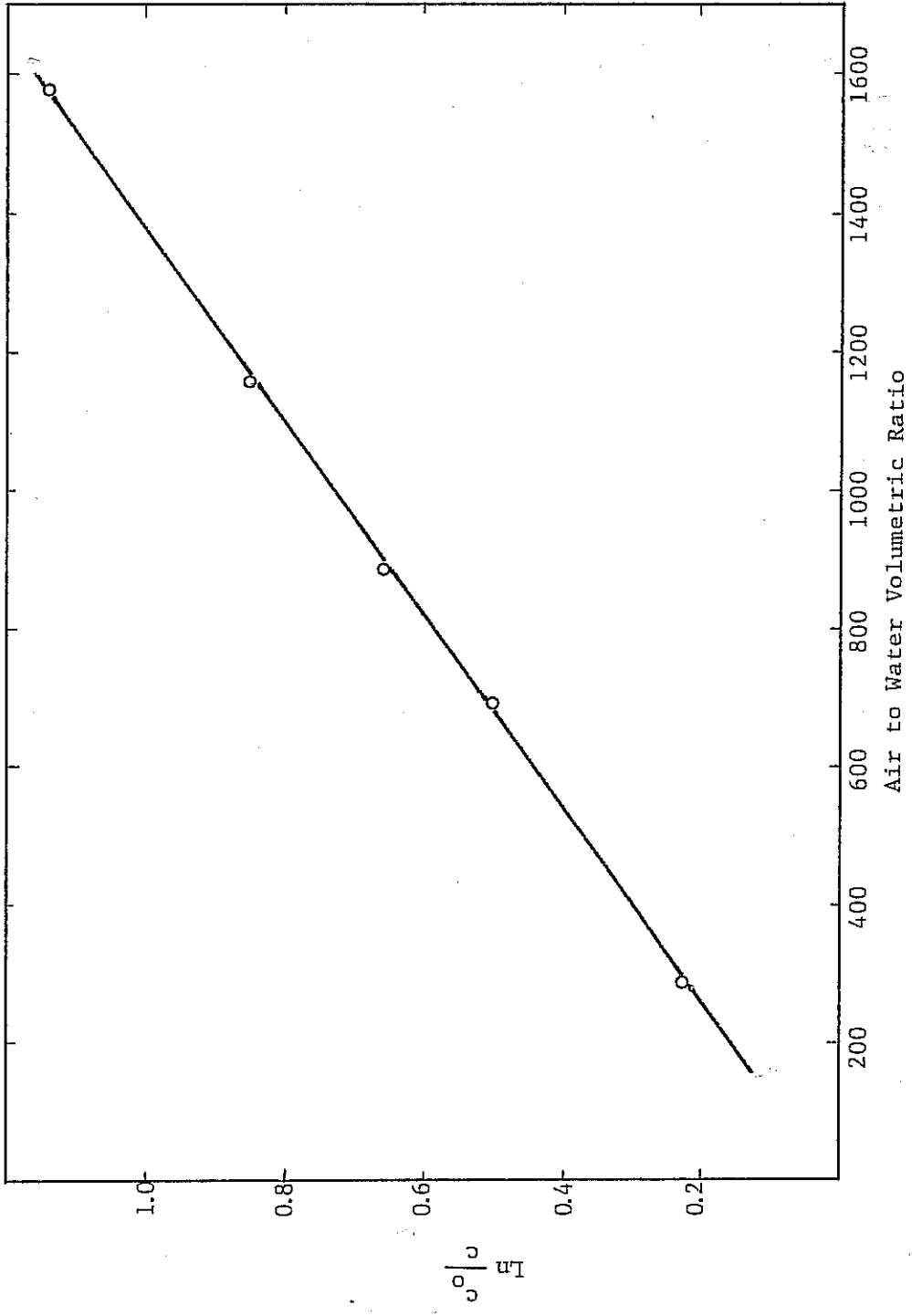


Figure 12. Dependence Between Air to Water Volumetric Ratio and Degree of Ammonia removal (Run 28)

TABLE 4
 BASIC PARAMETERS AND RESULTS OF THE EXPERIMENTS
 RUNS 1-9, 29, FINE BUBBLES

Run	Air Flow l/min	Water Volume l	Diffuser Submersion cm	Slope ⁴ b $\times 10^4$	Standard Deviation on Slope ⁴ b $\times 10^4$
1	0.56	0.50	61.7	7.92*	0.187
2	0.65	1.0	46.7	7.01	0.086
3	0.60	0.50	23.4	6.42	0.069
4	0.60	0.20	9.3	7.06	0.223
5	0.60	0.20	9.3	6.80	0.071
6	0.58	0.25	11.5	6.56	0.076
7	0.60	0.10	4.5	6.56	0.081
8	0.27	2.0	94.4	7.26	0.121
9	0.27	1.0	46.3	6.62	0.142
29	0.58	0.06	2.6	7.18	0.061

*This value was discarded

TABLE 5
 BASIC PARAMETERS AND RESULTS OF THE EXPERIMENTS
 RUNS 10-15, MEDIUM SIZE BUBBLES

Run	Air Flow l/min	Water Volume l	Diffuser Submerston cm	Slope b $\times 10^4$	Standard Deviation on Slope b $\times 10^4$
10	1.08	1.0	47.0	6.61	0.103
11	1.00	0.50	22.6	6.95	0.039
12	1.11	0.50	22.9	7.05	0.107
13	1.14	0.25	10.7	7.02	0.213
14	1.08	0.15	5.6	7.54	0.033
15	1.35	0.10	3.4	6.91	0.056

TABLE 6

BASIC PARAMETERS AND RESULTS OF THE EXPERIMENTS
 RUNS 16-26, 28, COARSE BUBBLES

Run #	Air Flow l/min	Water Volume L	Diffuser Submersion cm	Slope b $\times 10^4$	Standard Deviation on Slope b $\times 10^4$
16	1.11	0.25	10.7	7.18	0.063
17	1.14	0.15	5.7	7.42	0.038
18	1.14	0.10	3.4	7.45	0.048
19	0.60	1.00	46.2	7.15	0.130
20	0.56	0.50	22.4	7.03	0.091
21	0.57	0.20	8.1	7.14	0.111
22	0.58	0.20	8.2	6.89	0.050
23	0.60	0.15	5.6	7.06	0.130
24	0.59	0.15	5.7	6.91	0.054
25	0.58	0.10	3.3	6.89	0.131
26	0.59	0.10	3.4	6.86	0.056
28	0.58	0.06	1.6	7.22	0.069

TABLE 7

BASIC RESULTS AND PARAMETERS OF THE
EXPERIMENTS WITH SURFACE AERATION

Run #	Hydraulic Conditions	Air Flow l/min	Water Volume l	Slope b $\times 10^4$	Standard Deviation on Slope b $\times 10^4$	Air Saturation with Ammonia %
31	agitation, bubble formation	0.59	0.20	6.52	0.078	94
27	agitation, no bubble formation	0.58	0.20	5.32	0.153	77
30	no agitation, no bubble formation	0.58	0.20	4.28	0.126	62

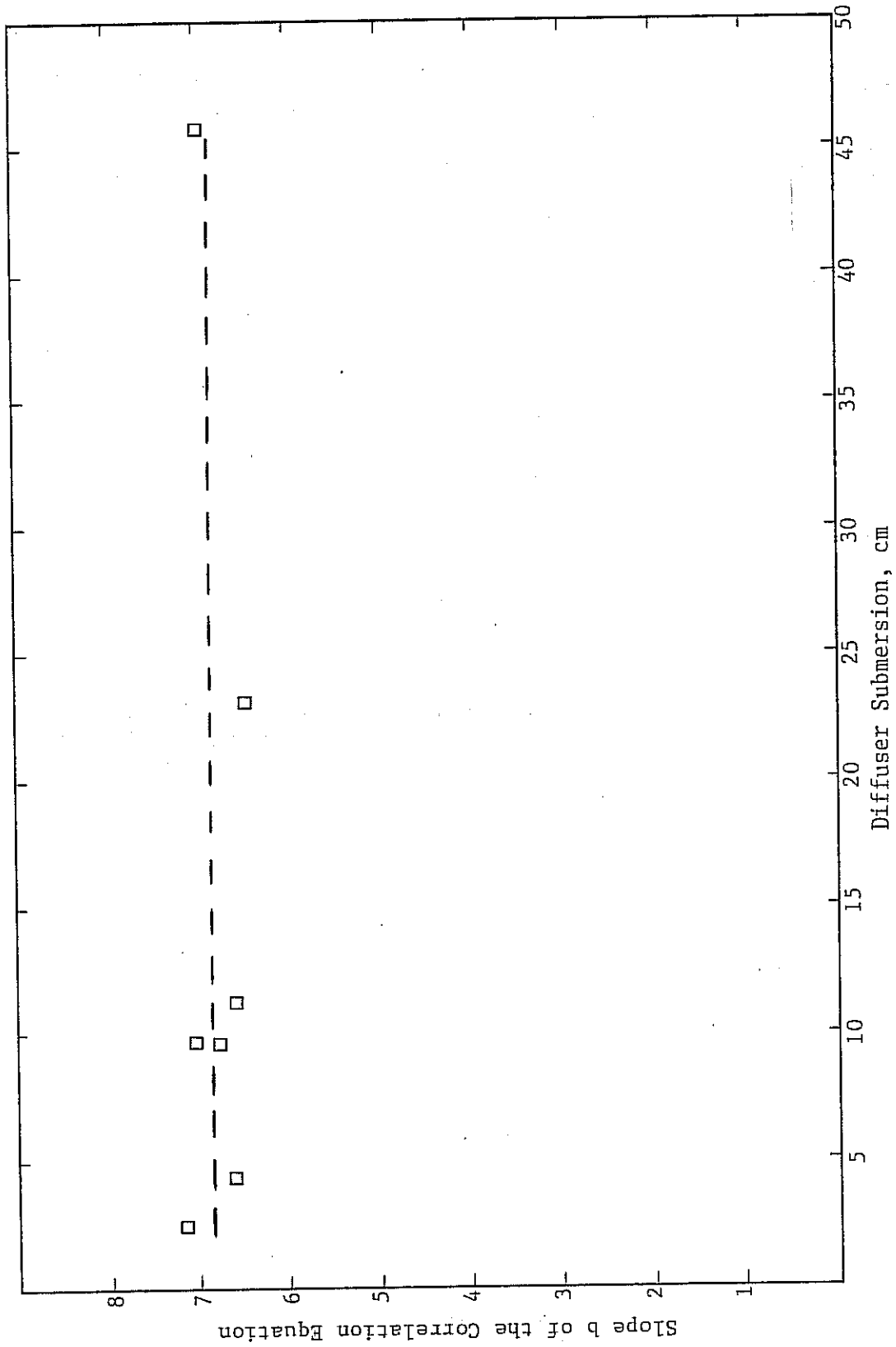


Figure 13. Dependence of the Slope of the Correlation Equation on Diffuser Submersion. Fine Bubbles, Flow 0.60 l/min

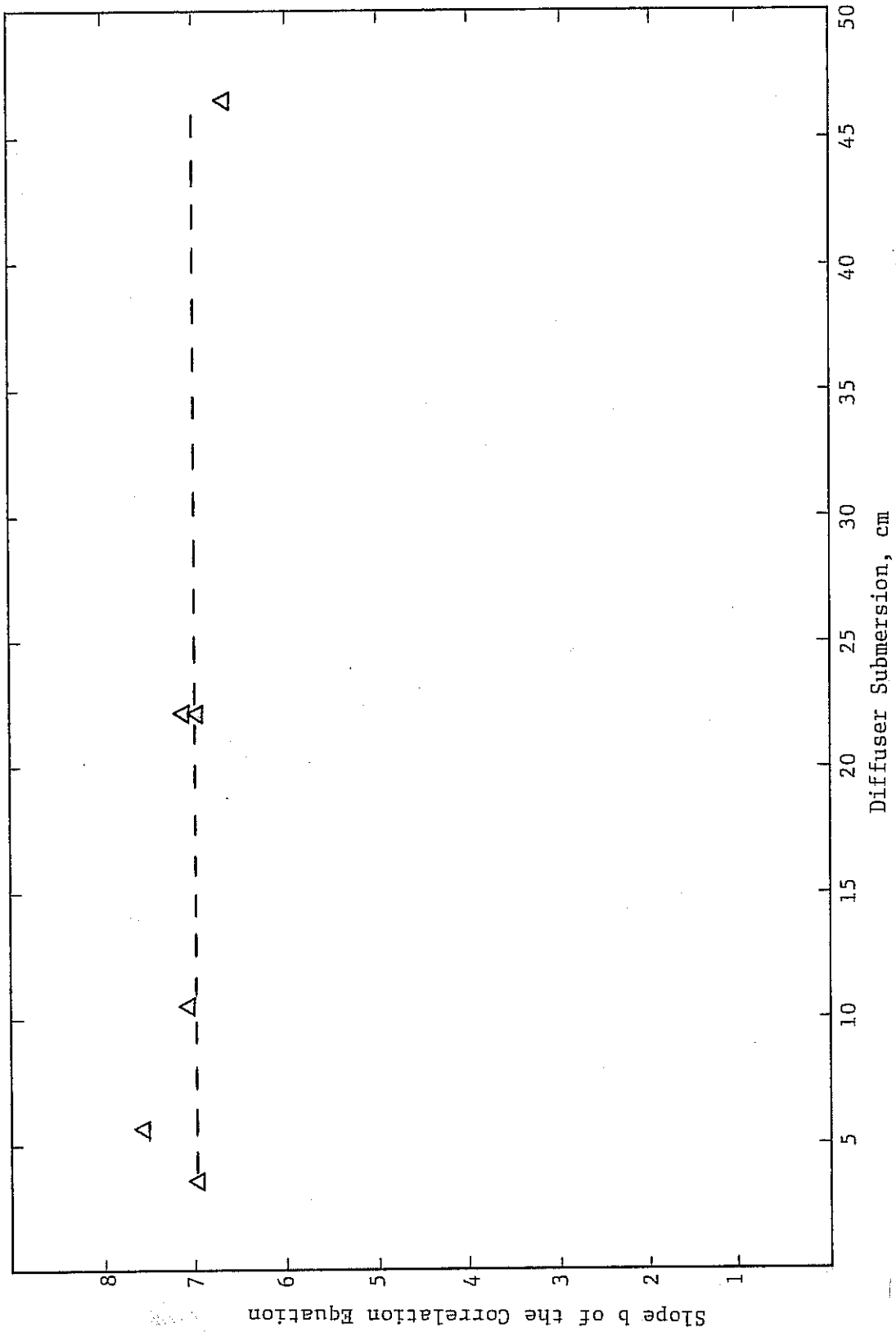


Figure 14. Dependence of the Slope of the Correlation Equation on the Diffuser Submersion. Medium Bubbles, Flow 1.10 l/min

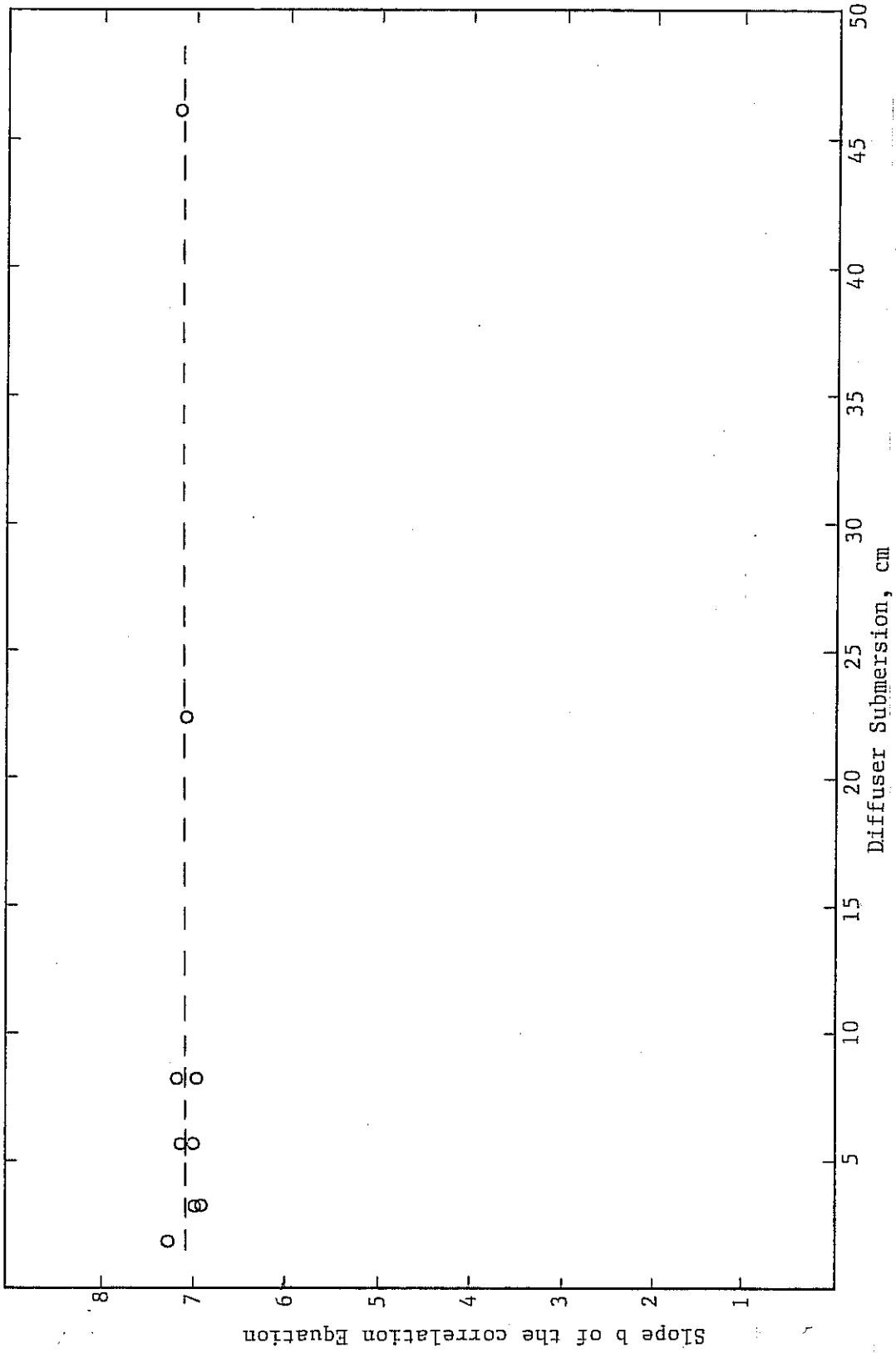


Figure 15. Dependence of the Slope of the Correlation Equation on the Diffuser Submersion. Coarse Bubbles, Flow 0.60 l/min

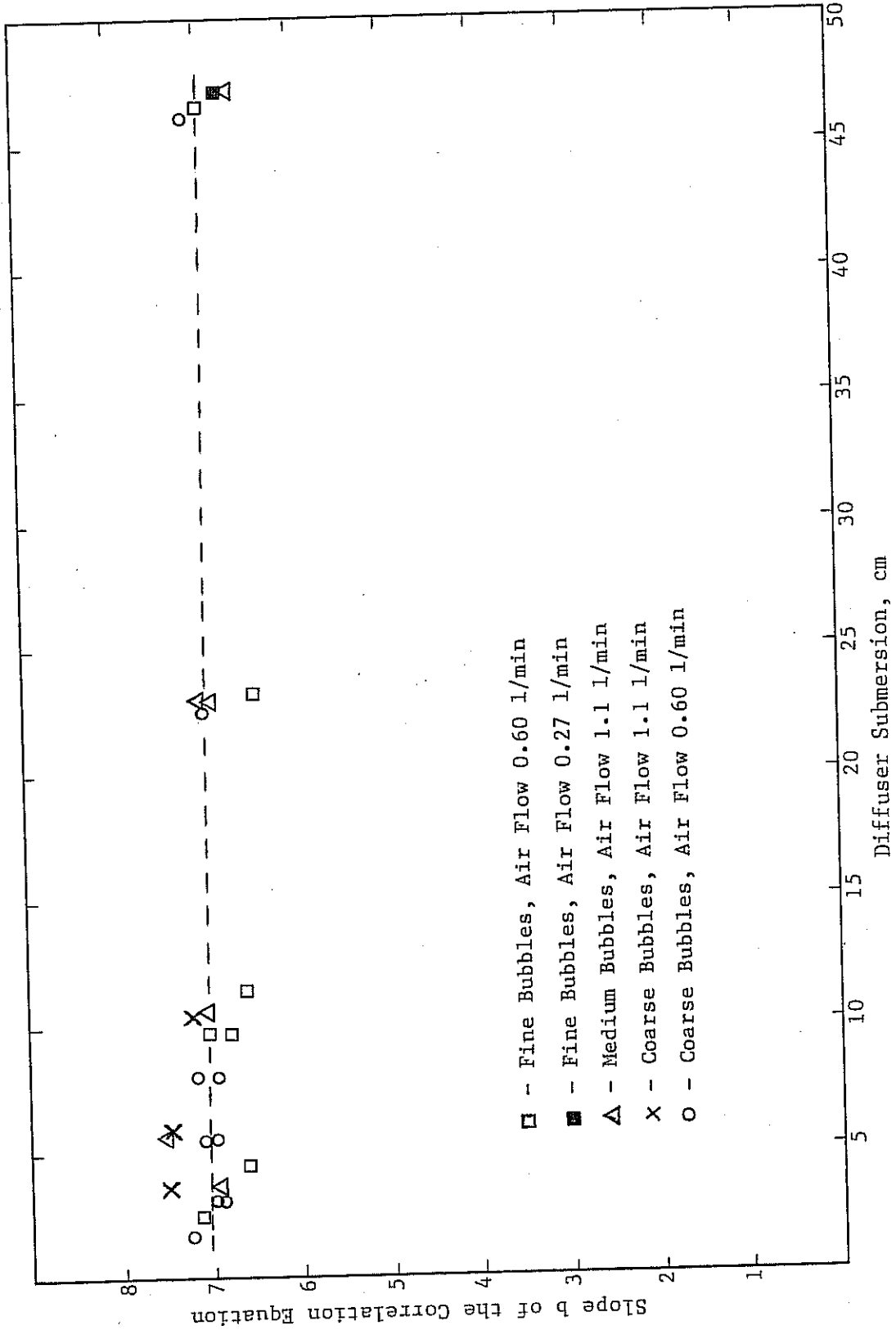


Figure 16. Dependence of the Slope of the Correlation Equation on the Diffuser Submersion. All Runs

CHAPTER VI

DISCUSSION

Surface effect

For the experiments with surface aeration only (without bubbling) $\tau=0$ and $f=0$. Therefore from Equations 28 and 29 we get

$$s/Q = \frac{b}{K \cdot P} \quad (31)$$

Values of the term s/Q calculated for three different mixing conditions, as shown in figures 10a, b and c are: 0.94, 0.77 and 0.62, respectively. This indicates, as expected, that s/Q is a function of the hydrodynamic conditions at the water-air interface. Comparison of these numbers with Equation 28 indicates that, even for $\exp(-a \cdot \tau)$ approaching 1, this surface effect provides significant saturation of the air with ammonia (with fraction of saturation equal to s/Q).

Effect of bubble diameter and contact time on rate of ammonia removal

According to Equations 28 and 29

$$b = K \cdot P \cdot \left[1 - (1 - s/Q) \cdot \exp\left(-\frac{6 \cdot d}{d} \cdot \tau\right) \right] \quad (32)$$

The term in brackets represents the effect of the mass transfer rate on the rate of ammonia removal. For a given bubble diameter d , the mass

transfer coefficient k_L can be assumed to be constant. For constant Q , hydrodynamic conditions over the water surface are similar and therefore s/Q can be assumed to be constant. Thus an increase in contact time τ should result in an increase of the slope b with its value reaching $K \cdot P$ for sufficiently high values of τ .

Inspection of Figures 13-15 indicates that there is no decrease in b with decreasing contact time (water level), even for bubbles with the largest diameter (Figure 15), where mass transfer limitations should be most easily seen. Figure 16 indicates that bubble diameters have no impact on the rate of ammonia removal. Values of the slope b for all bubble sizes, diffuser submersion and air flow rates are in the range $6.42 \cdot 10^{-4} - 7.54 \cdot 10^{-4}$. Comparison of these numbers with values of the equilibrium constant given in Table 2 indicates that no significant mass-transfer effect can be noted. (The value of P at 25°C and $\text{pH}=11.65$ is 0.996) Differences in the values of b appear to be due to experimental error only. In order to verify this a statistical analysis was performed.

According to Equation 32 the dependence between b and τ can be expected to be in the following linearized form:

$$\ln \frac{K \cdot P}{K \cdot P - b} = \frac{6 \cdot \tau}{d} - \ln(1 - s/Q) \quad (33)$$

If a correlation existed between mean bubble contact time τ and the term $\ln \frac{K \cdot P}{K \cdot P - b}$, the slope a $\left(a = \frac{6 \cdot \tau}{d} \right)$ of the correlation line would

be statistically different from zero. For our calculations the value for $K \cdot P$ has been taken as $7.3 \cdot 10^{-4}$, a value close to the upper limit of the experimental values. The results of the t-test performed on the significance of the slope a (Figures 17-19) are given in the Table 8. Detailed calculations are given in Appendix C.

The results indicate that the slope a is not significantly different from zero at the 90% confidence level (Table 8). This means that changes in the contact time in the range investigated during the experiments have no discernible effect on the term $[1 - (1-s/Q) \cdot \exp(-a \cdot \tau)]$, given the experimental precision achieved. So, even for coarse bubbles after a very short contact time corresponding to a water column height of only a few mm the term $(1-s/Q) \cdot \exp(-a \cdot \tau)$ is almost zero, and further increase in contact time does not have a measurable impact on the slope b . The surface term $(1-s/Q)$ has a damping effect on this results, diminishing it still further. From the results of the experiments on surface aeration, the value of s/Q can be assumed to be about 0.77 (continuous mixing with no bubble formation). Note that the value $s/Q=0.94$ was obtained with bubble formation on the water surface and therefore 0.94 is equal to the term $[1 - (1-s/Q) \cdot \exp(-a \cdot \tau)]$, rather than to s/Q alone. With this assumption the results of the statistical analysis indicate that \mathcal{A} is relatively large, so that even for the smallest contact times used, the term $(1-s/Q) \cdot \exp(-a \cdot \tau)$ is already close to zero.

It should be emphasized that the results of the above statistical analysis indicate only that b is essentially independent of τ . Rejection of the hypothesis that b is a function of τ makes the

TABLE 8

RESULTS OF THE CORRELATION BETWEEN
SLOPE b AND CONTACT TIME t

Bubble Size	Air Flow Range L/min	t-ratio for the Slope	# degree of Freedom ν	t for 90% and ν [22]	Is correlation significant at 90% confidence level?
Fine	0.58 - 0.65	-0.12	5	2.015	no
Medium	1.0 - 1.35	-1.43	3	2.353	no
Coarse	0.56 - 0.60	0.77	7	1.895	no

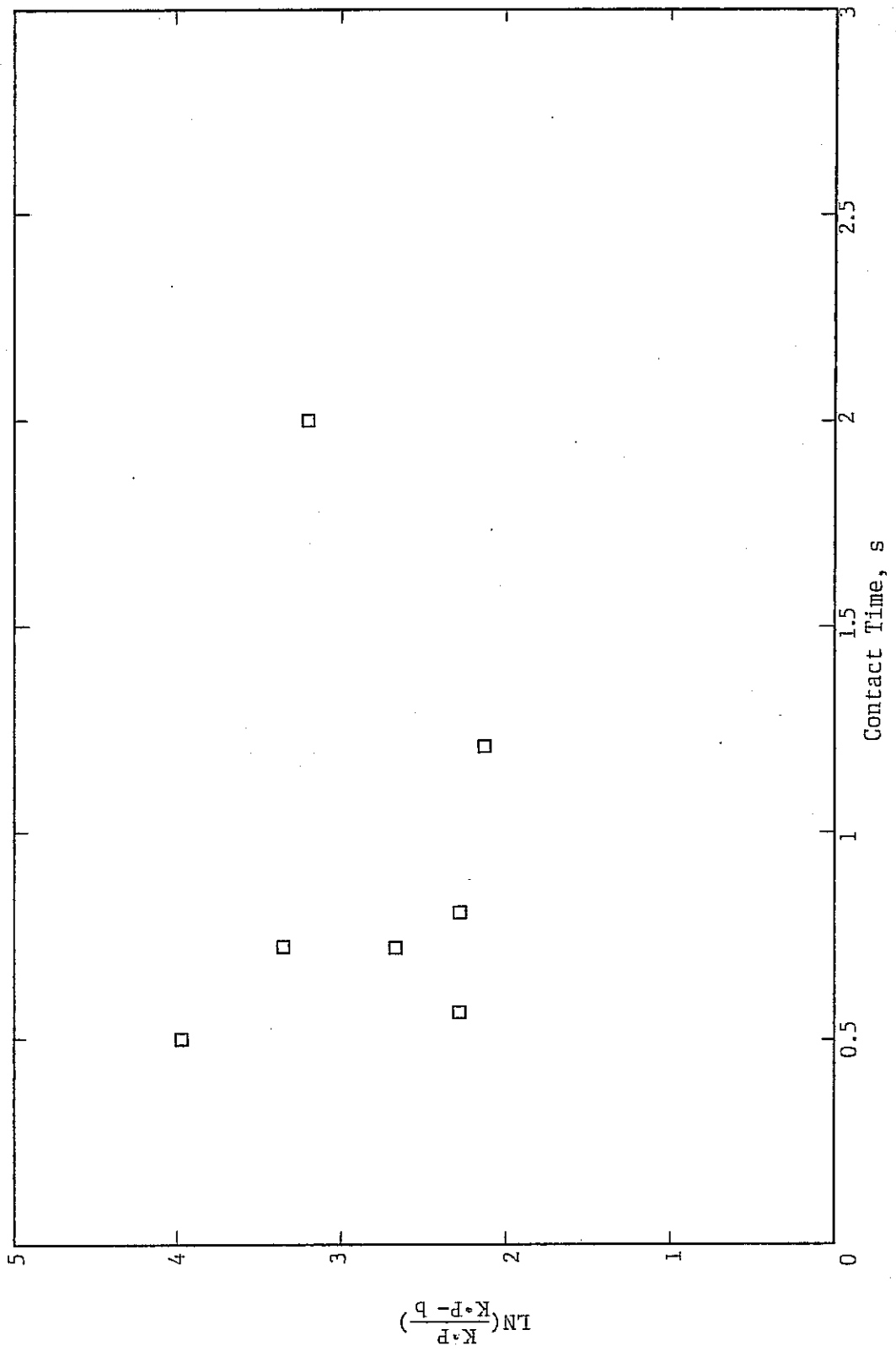


Figure 17. Effect of the Bubbles Contact Time on the Efficiency of Ammonia Removal
Fine Bubbles, Flow 0.60 l/min

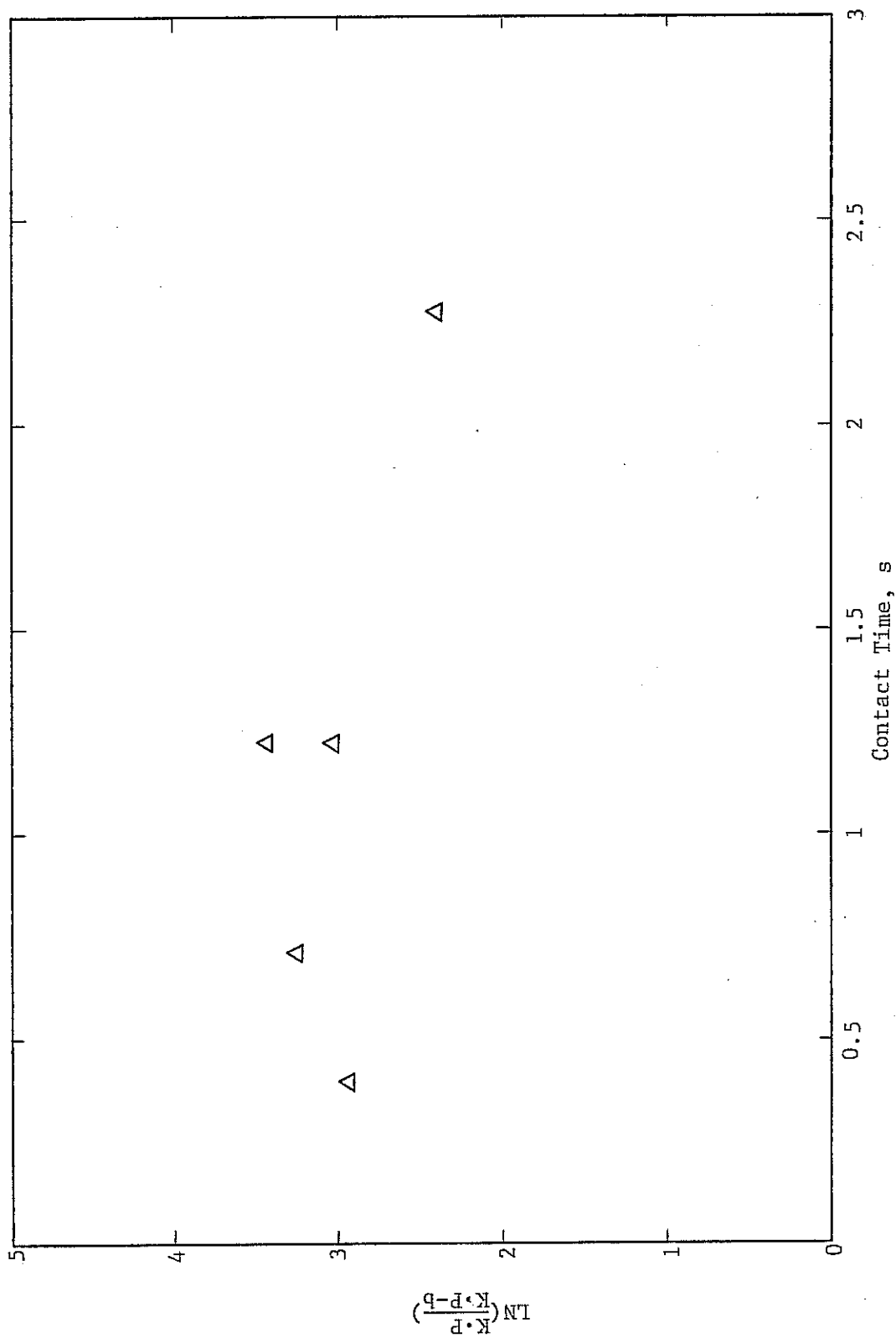


Figure 18. Effect of the Bubbles Contact Time on the Efficiency of Ammonia Removal Medium Bubbles, Flow 1.10 l/min

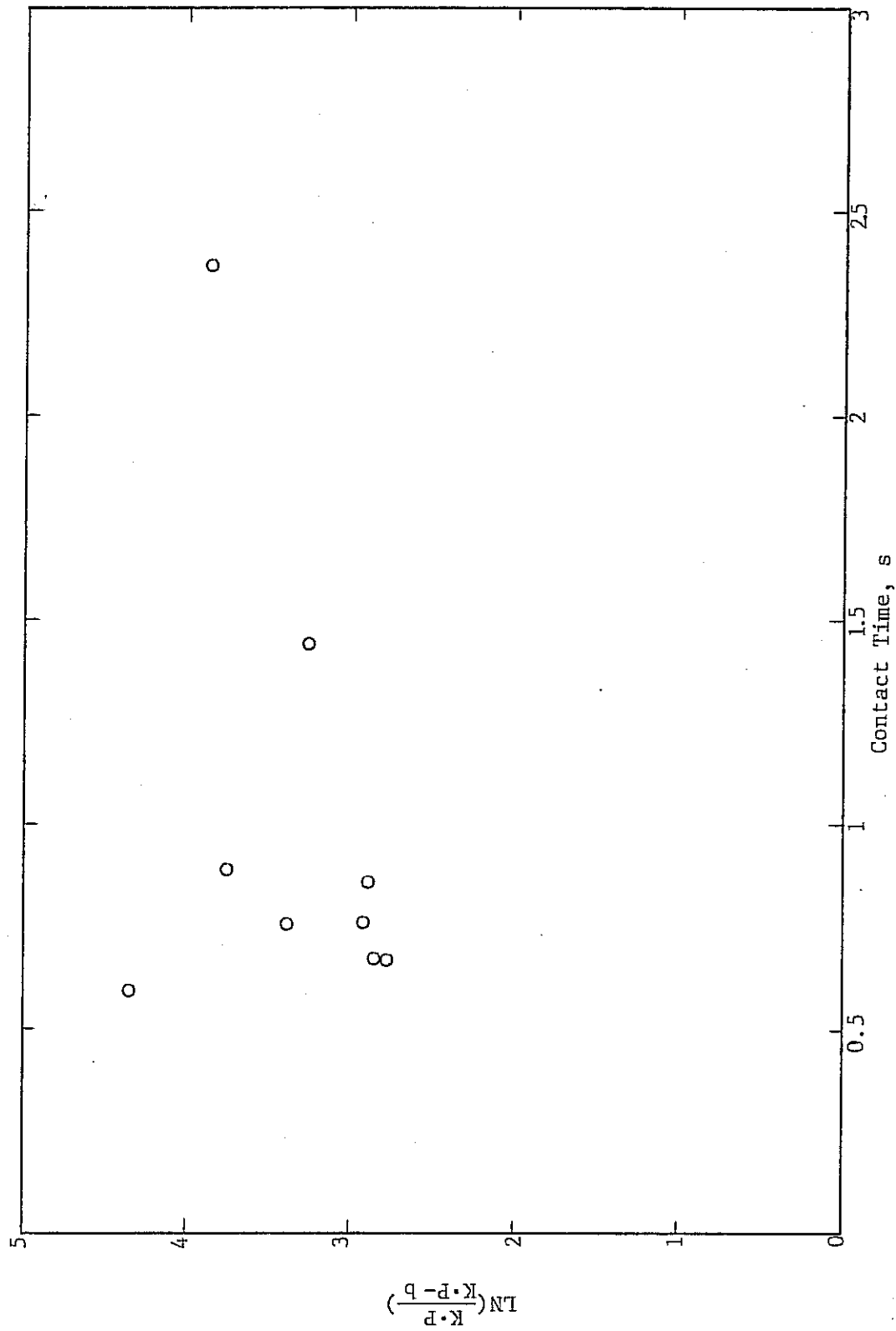


Figure 19. Effect of the Bubbles Contact Time on the Efficiency of Ammonia Removal
Coarse Bubbles, Flow 0.60 l/min

assumption that $KP=7.3 \cdot 10^{-4}$ is erroneous since KP is then equal to the mean experimental value of b , rather than to the upper bound for it. It follows that Equation 33 in the presented form can not be the basis for any numerical estimation of α . Thus the statement that the slope $a \left(a = \frac{6 \cdot \alpha C}{d} \right)$ is not significantly different from zero is only in apparent contradiction to the conclusion that α is too big to be measured experimentally; this point is clearer if one looks at Equation 32.

A practical conclusion is that for even coarse bubbles (6.2 mm) and minimal diffuser submersion, the rate of ammonia stripping is for all practical purposes entirely equilibrium and not mass transfer controlled. Air leaving the solution is saturated with ammonia. Therefore, in order to predict the rate of ammonia removal in a diffused aeration system (or to design it), it is enough to know the value of the equilibrium constant K and the fraction P of ammonia-nitrogen present as NH_3 (which is a function of pH and temperature).

This conclusion is at variance with some results reported in the literature (as discussed in the Chapter II). In particular findings by Shpirt [15] that an increase in bubble diameter and diffuser submersion depth improve the process efficiency seem to be erroneous. Also, such suggestions that for design purposes the mass transfer coefficient should be determined experimentally or estimated from semi-empirical correlations [14] are at variance with the findings of the present study.

From the results presented in this study it is apparent that changes in the ammonia-nitrogen concentration ($\text{NH}_4^+ + \text{NH}_3$) in a diffused aeration system can be calculated from the following equations:

$$c = c_o \cdot \exp \left(- K \cdot P \cdot \frac{Q \cdot t}{V} \right) \quad (34)$$

for batch operation, or

$$c = c_o \cdot \exp \left(- K \cdot P \cdot \frac{Q}{Q_L} \right) \quad (35)$$

for continuous operation, where Q_L is the water flow rate. Values for the equilibrium constant K are available in many sources, while P can be readily calculated from Equation 17.

Estimation of the mass transfer coefficient

The lower limit of the mass transfer coefficient α for a bubble rising through the water column can be estimated from the experimental data in this study.

Let us assume that a decrease in the slope b , due to mass transfer limitation, would be experimentally detected if its value was below the 95% confidence interval of the mean experimental value of b .

Therefore

$$b_m = \bar{b} - \delta \cdot t_{95\%} \quad (36)$$

where b_m = maximum value of b experimentally detected as different from $K \cdot P$

δ = standard deviation of b

\bar{b} = mean experimental value of b

If we assume that $K \cdot P$ is equal to the mean experimental value of b , Equation 17 can be rearranged into the form

$$\mathcal{C}_m = \left[\ln \frac{\bar{b}}{\bar{b} - b_m} + \ln(1 - s/Q) \right] \cdot \frac{d}{6\tau} \quad (37)$$

where \mathcal{C}_m is a lower limit of \mathcal{C} .

For our calculations, s/Q was taken as 0.77 which was the value obtained from the experiment on desorption from the stirred water surface. The minimal values of \mathcal{C} calculated from this equation are given in Table 9, column 6 (Detailed calculations are given in Appendix D). They should be considered rough estimates, due to the number of assumptions involved in the calculations. Actual values for \mathcal{C} must be higher than that calculated if a decrease in slope b is not detected with the experimental techniques applied.

The limiting values of \mathcal{C} , calculated in the above described manner, can be compared to the ones predicted theoretically. The latter values have been generalized (for any water-gas-air system) in the form of semiempirical formulas for the mass transfer coefficient for bubbles rising in the water. Detailed calculations are given in Appendix D and the results are shown in Table 9.

Comparison of columns 5 and 6 in Table 9 indicates, that there is no contradiction between values for the mass transfer coefficient calculated theoretically and the limits of \mathcal{C} obtained experimentally.

TABLE 9

COMPARISON OF THEORETICALLY PREDICTED AND OBTAINED
VALUES OF MASS TRANSFER COEFFICIENTS

1	2	3	4	5	6
Bubbles Size mm	K_g cm/s	K_l cm/s	Ratio of Gas Film to Liquid Film Resistance	α Theoretically Predicted cm/s	Minimum Value of α Obtained from Experi- ments, α_m cm/s
Fine 0.35	38.3	0.135	51	32.0	0.016
Medium 4.2	3.19	0.039	177	3.17	0.271
Coarse 6.1	2.20	0.032	210	2.19	0.249

In column 4, Table 9, the ratio of the water phase to the gas phase resistance is given. This indicates that, even for the smallest bubbles used, virtually all resistance to mass flow is located in the gas phase. This is due to the high solubility of ammonia in water, which means that the mass of dissolved ammonia present in the bubble water boundary layer is adequate to essentially saturate a large volume of air without replenishment from the bulk solution. Therefore, to provide adequate mass transfer conditions, there is no need for an energy-consuming formation of a large air-water interfacial area.

From Equation 26, it can be calculated that at 25°C approximately $3300\text{m}^3\text{air}/\text{m}^3\text{water}$ is necessary to remove 90% of the ammonia, assuming no mass transfer limitations.

The above considerations indicate that constructions with very low resistance to air flow are preferred for ammonia desorption from water. Diffused aeration does not satisfy such requirements, and therefore its application to the ammonia removal seems to be of limited prospect.

CHAPTER VII

CONCLUSIONS

1. Desorption of ammonia from water by diffused aeration is equilibrium controlled for all technically feasible bubble sizes and depths of submersion. Air leaving the desorption column was saturated with ammonia.
2. The depth of submersion of the diffuser and the bubbles size have no impact on the efficiency of the process.
3. The rate of ammonia removal can be calculated readily from Equations 34 and 35. Thus, experimental investigations of the rate of ammonia removal and the derivation of empirical correlations for design purposes do not seem to be needed.
4. The percent of ammonia present in solution in undissociated form can be calculated from the following equation:

$$P = \frac{1}{1 + 10^{10.06 - \text{pH} - t \cdot 0.0329 - \log(f_1)}}$$

5. Values for the mass transfer coefficient, as estimated from the experimental results, are not in conflict with the ones theoretically predicted.
6. Due to the mass-balance and mass-transfer considerations, diffused aeration is not an economical process for ammonia removal. The large amounts of air required and rapid (gas-phase controlled) mass

transfer rate indicate that apparatus with very low resistance to air flow will be more economical.

APPENDIX A

COMPUTER PROGRAM FOR PROCESSING OF EXPERIMENTAL DATA

APPENDIX B

DETAILED PARAMETERS AND RESULTS OF RUNS NO. 3 AND 4

INITIAL AND AVERAGE DATA FOR THE RUN 3

CONC. [MG/L]	AV.FLOW [L/MIN]	TEMP. [CELS]	ABSORB.	PH	VOLUME [L]	DELTA VOL. [L]	LEVEL [CM]	DELTA PRES. [CM H2O]
16.68	.60	25.0	.570	11.64	0.50	.0085	23.4	4.2

DETAILED DATA AND RESULTS FOR THE RUN 3

SAMPLE NO	TIME [MIN]	AV.FLOW [L/MIN]	TEMP. [CELS]	ABSORB.	CONCENTRATION [MG/L]	X	Y
1	199.0	.615	25.4	.484	14.18	253.5	.1623
2	359.0	.608	25.3	.424	12.43	457.2	.2935
3	552.0	.603	25.2	.358	10.52	704.4	.4610
4	792.0	.590	25.3	.301	8.86	1011.8	.6323
5	1432.0	.570	25.2	.174	5.17	1816.0	1.1708

INITIAL AND AVERAGE DATA FOR THE RUN 4

CONC. [MG/L]	AV.FLOW [L/MIN]	TEMP. [CELL]	ABSORB.	PH	VOLUME [L]	DELTA VOL. [L]	LEVEL [CM]	DELTA PRES. [CM H2O]
43.26	.60	25.0	1.485	11.61	0.20	.0035	9.5	3.8

DETAILED DATA AND RESULTS FOR THE RUN 4

SAMPLE NO	TIME [MIN]	AV.FLOW [L/MIN]	TEMP. [CELL]	ABSORB.	CONCENTRATION [MG/L]	X	Y
1	118.0	.601	25.0	1.051	30.65	373.1	.3446
2	247.0	.598	25.5	.801	23.39	781.8	.6150
3	356.0	.581	25.4	.633	18.51	1122.1	.8491
4	455.0	.603	25.4	.518	15.17	1448.5	1.0482
5	547.0	.590	25.4	.415	12.17	1751.1	1.2680

APPENDIX C

CALCULATION OF BUBBLE CONTACT TIME AND IT'S
CORRELATION WITH SLOPE b

Fine Bubbles

For runs 2-7 and 29 with fine bubbles and average flow 0.60 l/min, the volume of the air in the column (ΔH) corresponding to the given water level (diffuser submersion) was read from Figure 4. The average bubble contact time (τ) for flow $Q = 0.60$ l/min and the column cross section area $A = 21.2$ cm² can be calculated from the following equation:

$$\tau = \Delta H \frac{A}{Q} = \Delta H(\text{cm}) \cdot \frac{21.2(\text{cm}^2) \cdot 60(\text{s/min})}{0.60(\text{l/min}) \cdot 1000(\text{cm}^3/\text{l})} = \Delta H(\text{cm}) \cdot 2.16 \quad (\text{s})$$

For the seven runs mentioned above, the values for τ and $\ln \frac{K \cdot P}{K \cdot P - b}$ were correlated yielding the following equation:

$$\ln \frac{K \cdot P}{K \cdot P - b} = 2.91 - 0.0672 \cdot \tau$$

The standard deviation of the slope is 0.582 and thus t-ratio for the slope of the above equation equals

$$- \frac{0.0672}{0.582} = - 0.12$$

Medium Bubbles

The same procedure was applied to runs 10-13 and 15 with an average flow 1.1 l/min. Using Figure 5 for determination of ΔH , we find that τ can be calculated from the following equation:

$$\tau = \Delta H(\text{cm}) \cdot \frac{21.2(\text{cm}^2) \cdot 60(\text{s}/\text{min})}{1.1(\text{l}/\text{min}) \cdot 1000(\text{cm}^3/\text{l})} = \Delta H(\text{cm}) \cdot 1.16 \quad (\text{s})$$

The resulting correlation is as follows:

$$\ln \frac{K \cdot P}{K \cdot P - b} = 3.39 - 0.35 \cdot \tau$$

$$t\text{-ratio} = \frac{-0.35}{0.245} = -1.43$$

Coarse Bubble

For runs 19-26 and 28 with average flow 0.6 l/min τ can be calculated as

$$\tau = \Delta H(\text{cm}) \cdot \frac{21.2(\text{cm}^2) \cdot 60(\text{s}/\text{min})}{0.60(\text{l}/\text{min}) \cdot 1000(\text{cm}^3/\text{l})} = \Delta H(\text{cm}) \cdot 2.12 \quad (\text{s})$$

Values for ΔH were read from Figure 6, and correlation equation has form

$$\ln \frac{K \cdot P}{K \cdot P - b} = 3.07 + 0.272 \cdot \tau$$

$$t\text{-ratio} = \frac{0.272}{0.351} = 0.77$$

APPENDIX D

CALCULATION OF THE MASS TRANSFER COEFFICIENT

Calculation of the minimum value of the mass transfer coefficient

According to Equation 37

$$\alpha_m = \left[\ln \frac{\bar{b}}{b - b_m} + \ln(1 - s/Q) \right] \cdot \frac{d}{6 \cdot \tau}$$

The mean experimental value of the slope is $\bar{b} = 6.92 \cdot 10^{-4}$ with standard deviation $\delta = 0.219 \cdot 10^{-4}$. One sided, 95% confidence limit on b is equal to

$$b_m = \bar{b} - \delta \cdot t_{95\%} = 6.92 \cdot 10^{-4} - 0.219 \cdot 10^{-4} \cdot 1.703$$

$$b_m = 6.55 \cdot 10^{-4}$$

The value of s/Q was assumed as equal to that obtained from run 29 (agitation without bubbles formation), $s/Q = 0.77$. Therefore

$$\alpha_m = \left[\ln \left(\frac{6.92}{6.92 - 6.55} \right) - 1.46 \right] \cdot \frac{d}{6 \cdot \tau} = 1.47 \cdot \frac{d}{6 \cdot \tau}$$

The shortest contact times applied in experiments were (see Appendix C)

for fine bubbles ($d = 0.32$ mm) $\tau = 0.49$ s

for medium bubbles ($d = 4.2$ mm) $\tau = 0.38$ s

for coarse bubbles ($d = 6.1$ mm) $\tau = 0.60$ s

Substitution yields

$$\text{for fine bubbles} \quad \alpha_m = 1.47 \cdot \frac{0.032 \text{ cm}}{6 \cdot 0.49 \text{ s}} = 0.016 \text{ cm/s}$$

$$\text{for medium bubbles} \quad \alpha_m = 1.47 \cdot \frac{0.42 \text{ cm}}{6 \cdot 0.38 \text{ s}} = 0.271 \text{ cm/s}$$

$$\text{for coarse bubbles} \quad \alpha_m = 1.47 \cdot \frac{0.61 \text{ cm}}{6 \cdot 0.60 \text{ s}} = 0.249 \text{ cm/s}$$

Calculation of the Theoretically Predicted Value of the Mass Transfer Coefficient

From the Lewis and Whitman two-film theory [23], the overall mass transfer coefficient k_c (gas phase based) is equal to

$$\frac{1}{k_c} = \frac{K}{k_L} + \frac{1}{k_g}$$

where K = equilibrium constant

k_L = liquid phase mass transfer coefficient

k_g = gas phase mass transfer coefficient

The value for k_L , for the gas-bubble liquid system can be calculated from the following semiempirical relationship [24]:

$$Sh = 1.1 \cdot Re^{0.5} \cdot Sc^{0.5}$$

where $Re = \frac{u \cdot d \cdot \rho_L}{\mu}$

u = bubble velocity

d = bubble diameter

ρ = density of the liquid

μ = absolute viscosity of the liquid

$$Sc = \frac{\mu}{\rho \cdot D_{NH_3-H_2O}}$$

$D_{NH_3-H_2O}$ = diffusivity of ammonia in the water

$$Sh = \frac{k_L \cdot d}{D_{NH_3-H_2O}}$$

For fine bubbles numerical values of these parameters are as follows:

$$\begin{aligned}
 u &= 0.28 \text{ m/s} \quad (\text{calculated from Figure 4}) \\
 d &= 3.5 \cdot 10^{-4} \text{ m} \\
 \rho &= 998 \text{ kg/m}^3 \\
 \mu &= 0.96 \cdot 10^{-3} \text{ kg/m}\cdot\text{s} \\
 D_{\text{NH}_3\text{-H}_2\text{O}} &= 1.76 \cdot 10^{-9} \text{ m}^2/\text{s}
 \end{aligned}$$

Thus

$$\text{Re} = \frac{0.28 \text{ (m/s)} \cdot 3.5 \cdot 10^{-4} \text{ (m)} \cdot 998 \text{ (kg/m}^3\text{)}}{0.96 \cdot 10^{-3} \text{ (kg/m}\cdot\text{s)}} = 102$$

$$\text{Sc} = \frac{0.96 \cdot 10^{-3} \text{ (kg/m}\cdot\text{s)}}{998 \text{ (kg/m}^3\text{)} \cdot 1.76 \cdot 10^{-9} \text{ (m}^2\text{/s)}} = 547$$

$$\text{Sh} = 1.1 \cdot \text{Re}^{0.5} \cdot \text{Sc}^{0.5} = 1.1 \cdot (102 \cdot 547)^{0.5} = 260$$

$$k_L = \frac{\text{Sh} \cdot D}{d} = \frac{260 \cdot 1.76 \cdot 10^{-9} \text{ (m}^2\text{/s)}}{3.5 \cdot 10^{-4} \text{ (m)}} = 1.31 \cdot 10^{-3} \text{ (m/s)}$$

For medium bubbles $u = 0.23 \text{ m/s}$, $d = 0.0042 \text{ m}$ and for coarse bubbles $u = 0.25 \text{ m/s}$ and $d = 0.0061 \text{ m}$. Values of k_L calculated in the same manner as for fine bubbles are

$3.4 \cdot 10^{-4} \text{ m/s}$ for medium bubbles and

$2.95 \cdot 10^{-4} \text{ m/s}$ for coarse bubbles

Value of the gas-phase mass transfer coefficient can be estimated from the theoretical equation derived under assumption that in the gas bubble molecular diffusion is the mechanism of mass transfer [25]

$$Sh = \frac{k_g \cdot d}{D_{NH_3-air}} = 6.6$$

where D_{NH_3-air} is diffusivity of ammonia in the air, equal to

$2.03 \cdot 10^{-5}$ m/s [25]. Thus, for fine bubbles

$$k_g = \frac{6.6 \cdot D_{NH_3-air}}{d} = \frac{6.6 \cdot 2.03 \cdot 10^{-5} (m^2/s)}{3.5 \cdot 10^{-4} (m)} = 0.38 (m/s)$$

For medium and coarse bubbles calculations yield $k_g = 0.032$ m/s and 0.022 m/s, respectively. Since bubbles rising in the water undergo deformations with resulting turbulent conditions inside the bubbles, the values calculated above are conservative ones.

Assuming for K a value $7.06 \cdot 10^{-4}$ we find that the overall mass transfer coefficient for fine bubbles is

$$\alpha = \frac{1}{\frac{K}{k_L} + \frac{1}{k_g}} = \frac{1}{\frac{7.06 \cdot 10^{-4}}{1.31 \cdot 10^{-3} (m/s)} + \frac{1}{0.38 (m/s)}} = 31.6 (cm/s)$$

For medium and coarse bubbles the respective values are 3.0 cm/s and 2.1 cm/s

The values of $\frac{K}{k_L}$ and $\frac{1}{k_g}$ in the equation above represent

the contributions of the liquid and gas phase resistance to the total resistance to the mass flow.

BIBLIOGRAPHY

1. "Process Design Manual for Nitrogen Control". U.S. Environmental Protection Agency, 1975 .
2. Wilson, R. W., et al., "Design and Cost Comparison of Biological Nitrogen Processes". Jour. Water Poll. Control Fed. Vol. 53, No. 8, 1975
3. Gonzales, J. G., and R. L. Culp, "New Developments in Ammonia Stripping, Part One", Pub. Works, May 1973
4. O'Farrell, T.P., et al., "Nitrogen Removal by Ammonia Stripping", Jour. Water Poll. Control Fed., Vol. 44, No. 8, 1972
5. Trulsson, Sven-Gunnar, "Ammonia Recovery From Wastewater in Packed Columns", Jour. Water Poll. Control Fed., Vol. 51, No. 10, 1979
6. Davies, T. H., and S. Y. Ip, "The Droplet Size and Height Effect in Ammonia Removal in a Spray Tower" Water Research, Vol. 15, No. 5, 1981
7. Idelovitch, E., and M. Michail, "Nitrogen Removal by Free Ammonia Stripping from High pH Ponds", Jour. Water Poll. Control Fed., Vol. 53, No. 9, 1981
8. Bennenworth, N. E., and N. G. Moris, "Removal of Ammonia by Air Stripping", Water Poll. Control Vol. 71, No. 5, 1972
9. van Vuuren, L. R. J., et al., "Current Status of Water Reclamation at Windhoek", Jour. Water Poll. Control Fed., Vol. 52, No. 4 1980
10. Slechta, A. F., and G. L. Culp, "Water Reclamation Studies at the South Tahoe Public Utility District", Jour. Water Poll. Control Fed., Vol. 39, No. 5, 1967
11. Argo, D. G., "Cost of Water Reclamation by Advanced Wastewater Treatment", Jour. Water Poll. Control Fed., Vol. 52, 1980
12. Downing, A. L., "Aeration in Relation to Water Treatment", Proc. Soc. Wat. Treat. Exam. Vol. 7, 1958
13. Bayley, R. W., "Desorption of Waste-Water Gases in Air", Effl. and Water Trt. Jour. (London), Vol. 7, 1967

14. Srinath E. G., and R. C. Loehr "Ammonia Desorption by Diffused Aeration", Jour. Water Poll. Control Fed., Vol. 46, No. 8, 1974
15. Shpirt E. "Role of Hydrodynamic Factors in Ammonia Desorption by Diffused Aeration", Water Res., Vol. 15, No. 6, 1981
16. "Lange's Handbook of Chemistry" 12th Ed. Edited by John A. Dean. MacGraw-Hill Book Company, 1979
17. "Chemical Engineers' Handbook", 5th Ed., Edited by R. H. Perry and C. H. Chilton, MacGraw-Hill Book Company, 1973
18. Trussel, R. P., "The Percent Un-Ionized Ammonia in Aqueous Ammonia Solution at Different pH Levels and Temperatures", Jour. Fisheries Research Board of Canada, Vol. 29, No. 10, 1972
19. Eckenfelder, W. W. Jr., "Principles of Water Quality Management", CBI Publishing Company, Inc., Boston, Ma, 1980
20. "Tri-Flat Variable Area Flowmeters" - Handbook no 10A9010, Fisher and Porter Co., Warminster, Pa.
21. "Standard Methods For the Examination of Water and Wastewater", 13th Ed. APMA-AWWA-WPCF, 1980
22. Kennedy, John B. and Adam M. Neville, "Basic Statistical Methods for Engineers and Scientists", 2nd Ed., Harper and Row, Publishers, New York, N.Y., 1976
23. Treybal, Robert E., "Mass-Transfer Operations", 3rd Ed., McGraw-Hill Book Company, 1980
24. Serwinski, M., "Zasady Inzynierii Chemicznej", 1st Ed., WNT, Warszawa, 1971
25. Hobler, T., "Dyfuzyjny Ruch Masy i Absorbery", 2nd Ed., WNT, Warszawa, 1976